NORTHWESTERN UNIVERSITY

Sub-diffusion and Compartmentalization: How the Nuclear Pore Complex and Stochastic Movement are Utilized to Dynamically Organize the Eukaryotic Genome

A DISSERTATION

SUBMITTED TO THE GRADUATE SCHOOL

IN PARTIAL FULFILLMENT OF THE REQUIREMENTS

For the degree

DOCTOR OF PHILOSOPHY

Field of Interdisciplinary Biological Sciences

By
Michael Chas Sumner

EVANSTON, ILLINOIS

September 2021

ABSTRACT

In nearly all Eukaryotes, the membrane-enclosed nucleus contains the vast majority of the cellular genome. Within this sub-cellular compartment, the nuclear architecture facilitates genomic chromatin organization. Controlling chromosomal loci's spatial positioning relative to subnuclear structures and each other can have local and global effects on gene expression. Moreover, chromatin organization can vary widely between species and even tissues within a multicellular organism. Determining how genes organize to establish and maintain transcriptional states is necessary for understanding this ancient, conserved method for epigenetic expression regulation. Within *Saccharomyces cerevisiae*, commonly known as brewer's yeast, hundreds of genes are known to interact with the Nuclear Pore Complex, become organized at the periphery, and form clusters of similarly regulated genes. Tracking these organized genes reveals that chromatin association with the Nuclear Pore Complex is dynamic and positioning at the nuclear periphery is the product of repetitive binding and disassociation events. Furthermore, inter-chromosomal gene clusters appear to coordinate movement vectors between loci through a mechanism that is still being elucidated. Dynamic repositioning between sub-nuclear compartments also occurs through a largely stochastic mechanism that relies on sub-diffusive gene locus movement, random collision with the Nuclear Pore Complex or other nuclear architecture, and momentary but repeated binding between the two elements. Developing a modular and widely applicable model for gene movement within Eukaryotes has allowed for simulating locus trajectories, generating better hypotheses for organizational mechanisms, and predict stochastic movement given conditions only achievable *in silico*. Taken together, this work explains how stochastic movement is sufficient for establishing dynamic gene positioning in the yeast nucleus and lays the foundation for further understanding more complex genome organization phenomena that impact the transcriptome and proteome.

ACKNOWLEDGMENTS

Jason and Donna Brickner, the giants upon whose shoulders I stand. There are so many ways this work would have been impossible without your mentorship and professional guidance. You are both inspirations for scientific dedication that most only hope to achieve.

Carlo Randise-Hinchliff, **Agustina D'urso**, and **Varun Sood** were some of the best PhD student advisors I could have asked for. You set the bar very high for scientific aptitude and cultivating a healthy work environment.

Atsushi Satomura and **Rob Coukos**, two of the best biologists I had the pleasure of working alongside, and the honor of being their friend.

All the members of the **Lackner Lab (Laura Lackner, Antoineen, Heidi), Reza Vafabakhsh,** and **Alec Wang** for all their help and rigorous discussion.

Katherine Berman, **Alexis Reyes**, and **Julie Liang**, thank you for being amazing colleagues and friends who were always open for rigorous discussion or pleasant stories over hot drinks.

Steven Torrisi, despite our distance, we have only deepened our intellectual bond and friendship. No amount of thanks is enough for your contributions to my research and personal development.

Dan O'Brien, thank you for the unquantifiable amount of advice you have given me and always reaching out. To me, you are a beacon of kindness and passion.

Julia Kent, **Big Rob R**., **Big Jon S**., **Big (Sweet) T**, **Enrique R**., **Val P**., **Ruka M**., **Ayush S**., **Tarif H**., and all from University of Rochester who showed me the importance of friendship, seeking knowledge, and understanding truth.

Cheeptip Benyajati and **Ethan David Cohen**, you both believed in me when few professors would, and I needed someone to help me see my own capabilities. I cannot thank you enough for the encouragement and opportunities you afforded to me.

My cousins **Krystyn**, **Kevin**, **Kellye**, **Michelle**, **Brian**, **Rachel**, **Daniel**, and **Jonathon**, while time and a pandemic have put distance between us, I hope we can all embrace each other soon.

Uncle Dan, **Aunt JoanE**, **Aunt Judy**, and **Uncle Bruce**, you've all done so much to help shape me into the person I am today. Thank you for being my biggest supporters since I was born.

Thank you and I love you all!!!

DEDICATION

My work herein has been dedicated to:

Bette Jane Sumner and **Charles Sumner** ~ Your endless love and support have made my life and all the good things in it possible. Thank you for your unwavering belief in me, encouraging me at every step, and giving me the confidence needed to succeed.

I love you both very much.

Zena Levan ~ My eternal companion and best friend.

You have loved me more than I ever knew possible. Your patience and kindness are boundless.

Thank you for helping me be the best person I can be, with you.

Ruby, our lab in the lab ~ The best contributor at any sub-group meeting.

I miss giving you belly scritches.

TABLE OF CONTENTS

		Page
1.	Abstract	3
2.	Acknowledgments	4
3.	Dedication	5
4.	List of Figures	7
5.	Chapter 1: Introduction	
	a. Nuclear Structure and Chromatin Organization	8
	b. The NPC as a Transcription Repressor	9
	c. The NPC as a Transcription Activator	12
	d. The NPC as an Epigenetic Memory Regulator	16
6.	Chapter 2: Transcription-Associated Peripheral Localization in Yeast	
	a. Determining Roles of TFs, Zip Code, and SAGA in Gene Localization	19
	b. Nucleoplasmic or Peripheral: Differences in Diffusive Movement	23
	c. Discussing the Components of Chromatin Diffusion Confinement	29
7.	Chapter 3: Quantifying and Modeling Gene Movement During Translocation and Clustering	
	a. Fractional Brownian Motion and Initial Simulations	31
	b. Simulating Interaction between Particle and Boundary	33
	c. Chromatin Dynamics During Repositioning	36
	d. Inter-Chromosomal Clustering	41
	e. Potential Mechanisms and Roles for Clustering	45
8.	Chapter 4: Conclusions and Future Directions	
	a. Connecting Position, NPC Interaction, and Transcription	46
	b. A Passive Process for Repositioning	47
	c. Interrogating the Clustering Mechanism	49
	d. Modeling Diffusion	51
9.	Materials and Methods	53

10. References 57

11. Vita 66

LIST OF FIGURES

PAGE

1.1 Spatial organization of nuclear pore complex (NPC) component interactions with chromatin. 10

1.2 Nuclear pore complex (NPC) proteins affect transcription. 13

1.3 Transcription-associated peripheral localization leads to inter-chromosomal clustering in yeast. 15

2.1 Transcription factor binding sites function as DNA zip codes, and most are dependent on SAGA function. 21

2.2 Different regulatory strategies lead to large-scale changes in nuclear organization over different time scales 22

2.3 Continuous and dynamic positioning at the nuclear periphery. 24

2.3 Mean-squared displacement (MSD) of chromatin sub-diffusion. 26

2.4 MSD of loci in cells that are predominantly peripheral or nucleoplamsic 27

2.5 Interaction with the NPC reduces chromatin sub-diffusion. 28

3.1 Comparison of simulations of sub-diffusion of nucleoplasmic chromatin. 32

3.2 Determining association and dissociation parameters for two-state model to best simulate NPC-interacting chromosomal loci 34

3.3 A fractional Brownian motion simulation of chromatin sub-diffusion. 35

3.4 Loss of Myo3 delays GRS I-dependent repositioning to the nuclear periphery. 37

3.5 Repositioning from the nucleoplasm to the NPC. 39

3.6 Dynamics of inter-chromosomal clustering. 42

3.7 Inter-chromosomal clustering leads to coordinated movement. 44

CHAPTER 1

INTRODUCTION

Portions of this chapter were published in:

Sumner, M.C. & Brickner J.H. 2021. The Nuclear Pore Complex as a Transcription Regulator. Cold Spring Harb Perspect Biol doi: 10.1101/cshperspect.a039438

And

Randise-Hinchliff, C, R Coukos, V Sood, MC Sumner, S Zdraljevic,, L Meldi Sholl, DG Brickner, S Ahmed, L Watchmaker, & JH Brickner (2016). Strategies to regulate transcription factor-mediated gene positioning and interchromosomal clustering at the nuclear periphery. The Journal of cell biology, 212(6), 633–646. doi:10.1083/jcb.201508068

NUCLEAR STRUCTURE AND CHROMATIN ORGANIZATION

Eukaryotic cells spatially organize their genomes in a nonrandom fashion that reflects and facilitates transcription regulation (Misteli 2020). Multiple imaging methods for metazoan nuclei are currently able to visualize the dense heterochromatin associated with the nuclear lamina at the nuclear periphery in many species and cell types (Fig. 1.1) (Jost, Bertulat and Cardoso 2012). Most metazoan cells position heterochromatin and other transcriptionally silent loci near the nuclear lamina and centromeric complexes, but this phenomenon can vary widely between organisms, tissue types, and even individual cells within a tissue to achieve different transcriptional effects (Falk, et al. 2019, Zykova, et al. 2018). In this way, metazoans utilize nuclear architecture like the lamina to organize and regulate their genomes. While most metazoans depend on nuclear lamina to facilitate nuclear structure, almost all unicellular Animal and Fungal organisms lack a constitutively expressed lamin protein. Though there is some evidence lamin-like proteins can be expressed under mechanical stress when adopting a multicellular-like state as in Dictyostelium (Batsios, et al. 2012). Lamins may be canonically synonymous with nuclear structure, but an even more ancient and ubiquitous protein complex has been shown to both facilitate genome organization and act as an epigenetic regulator of gene expression: the Nuclear Pore Complex (NPC).

In all Eukaryotes, the NPC has the primary role of selectively transporting cargo between the nucleoplasm and cytoplasm. Ubiquitous and essential, NPCs were discovered at a time when there was

still an ongoing debate about the existence of an organized nuclear membrane (Callan and Tomlin 1950) (Watson 1955). Work over the intervening decades has revealed NPC function, organization, mechanism, and structure (Gall 1967, Goldberg 1992, von Appen 2016). Approximately 30 unique proteins make up the core eightfold, radially symmetrical channel, with subcomplexes that extend from cytoplasmic and nucleoplasmic faces. In electron micrographs of metazoan nuclei, chromatin near NPCs appears less condensed than adjacent, lamin-associated heterochromatin leading to the notion that positioning of active genes near NPCs would enhance mRNA export and potentially transcription (Blobel 1985). Multiple biochemical methods have confirmed that many NPC proteins (known as “Nups”) physically associate with active genes, impacting the spatial organization of genes and gene expression (Brickner and Walter 2004, Casolari, Brown and Komili, et al. 2004, Guglielmi, Sakuma and D’Angelo 2020). Data from yeast, flies, and mammals indicates that Nup interactions alter gene expression to improve viability during stress conditions, maintain epigenetic memory of previous expression states, and promote tissue differentiation (Brickner, Cajigas, et al. 2007, Capelson, et al. 2010, Liang, et al. 2013, Lin 2019). In yeast, transcription factors (TFs) and Nups are known to interact with other complexes involved in mRNA export (i.e., TREX2 and Mex67), transcription/initiation (Mediator, SAGA histone acetyltransferase), and are generally required for establishment and maintenance of active gene targeting to the nuclear periphery (Dieppois 2006, Ahmed, et al. 2010, Jani 2014). In fact, repositioning and interaction of active genes with the yeast NPC can require multiple nucleoplasm-facing NPC proteins such as Nup1, Nup2, Nup60, Mlp1, and Mlp2 (Cabal, et al. 2006, Luthra, et al. 2007, Ahmed, et al. 2010, Light, Brickner, et al. 2010). Eukaryotic cells use NPCs and even soluble Nups as structural platforms for interaction between expression regulation complexes and chromatin through a wide variety of mechanisms, many of which we are only beginning to elucidate. (Ptak, Aitchison and Wozniak 2014)

THE NPC AS A TRANSCRIPTION REPRESSOR

The location of a gene on a chromosome can impact its expression; genes near centromeres or telomeres show reduced recombination and transcription, a phenomenon known as the “position effect” (Weiler 1995). Such position effects often reflect the spreading of silencing factors from initial recruitment

sites to sections of the chromosome with known protein-encoding genes (Gottschling 1990). For example, in budding yeast, telomeres localize at the nuclear periphery. Nuclear envelope membrane proteins and Nups that make up the inner and outer ring subcomplexes (i.e., Nup170, Nup145, and Nup60) act as a physical anchor to recruit and stabilize the Rap1/Sir2/Sir3/Sir4 complex, which binds telomeric-sequence DNA (Van de Vosse 2013, Lapetina 2017).

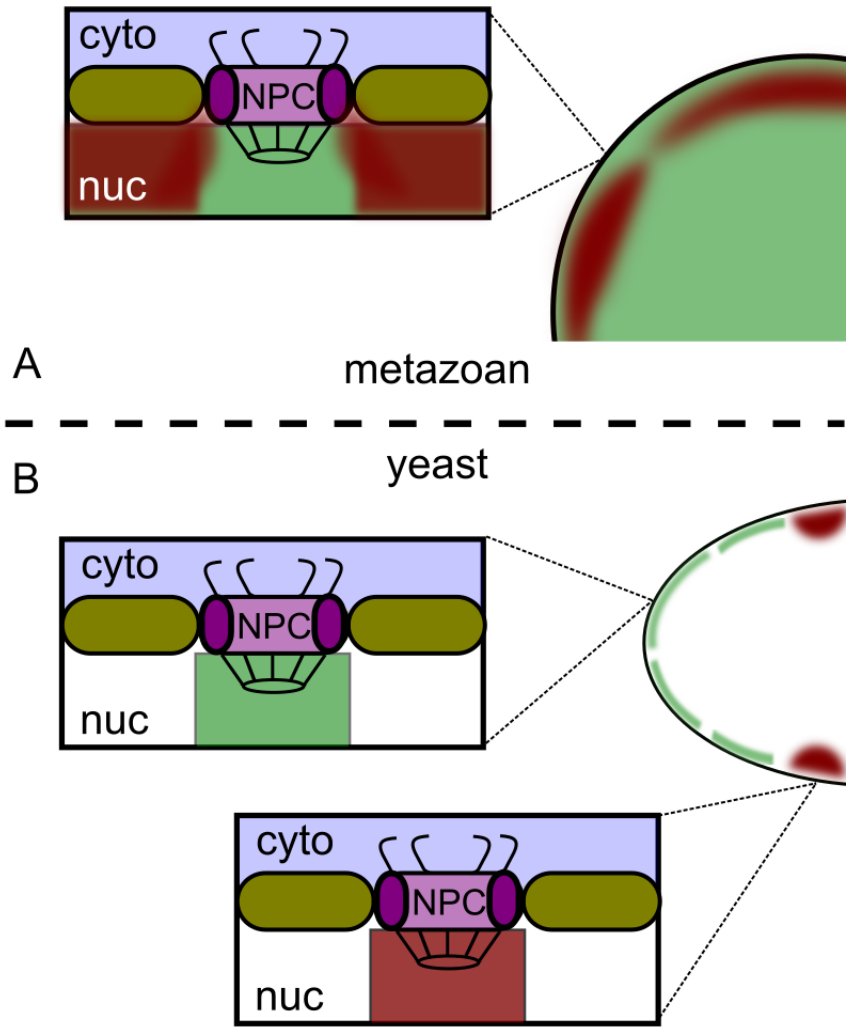

Figure 1.1 Spatial organization of nuclear pore complex (NPC) component interactions with chromatin. (A) (Right) Portion of metazoan nucleus where green represents euchromatin and red denotes heterochromatin. (Left) Peripheral chromatin adjacent to the nuclear lamina (red) and the NPC (green). (B) (Right) Portion of a Saccharomyces cerevisiae nucleus. Color indicates the space where NPC–chromatin interactions can occur (telomere silencing interactions in red, euchromatin transcription initiation in green). (Left) Insets show that the effects on transcription only occur at the nucleoplasmic face of the NPC.

The recruitment of Rap1 and the nuclear pore silencing factors Sir2, Sir3, and Sir4 (Fig. 1.2 A) (Gotta 1996) deacetylates histones and recruits more complexes to deacetylate neighboring chromatin. This feed-forward loop is responsible for establishing and maintaining silenced chromatin, and Rap1/Sir2/Sir3/Sir4 requires the NPC to stabilize itself on telomeres and to spread into sub-telomeric regions. Knocking out any of the Nups mentioned above leads to defects in the telomere silencing and other constitutively repressed sites like mating-type loci (Feuerbach 2002). In this way, the nuclear envelope and Nups contribute to both the spatial organization and transcriptional silencing of yeast telomeres.

In metazoan cells, there is a lot more variability in organizational potential as genes interact with both NPC-associated Nups at the nuclear periphery and soluble Nups localized throughout the nucleoplasm (Griffis 2002, Capelson, et al. 2010, Kalverda 2010, Liang, et al. 2013). At the fly NPC, active and silent genes interact with distinct Nups (Nup107 and Nup93, respectively) (Gozalo 2020). Polycomb repressive complexes (PRCs) catalyze methylation of H3K27 to establish and maintain facultative heterochromatin (Fig. 1.2 A). More than a third of Polycomb-associated domains also physically interact with Nup93. Compared to other Polycomb domains, those that interacted with Nup93 had increased PRC presence and were more likely to be positioned at the nuclear periphery (Gozalo 2020). Finally, Nup93 contributes to the transcriptional silencing of these regions. Thus, the interaction of Nups can also promote transcriptional silencing and heterochromatin formation in animals.

Nup interaction with the genome can also impact chromosome folding. Boundary elements and the chromatin architectural proteins that localize to them (CTCF and cohesion) interact with Nup153 to stabilize their organization in physical space and enhance insulation between topologically associated domains (TADs) (Fig. 1.2 B) (Kadota, et al. 2020). Knockdown of Nup153 leads to improper TAD formation and ectopic enhancer function across boundary domains. Embryonic stem cells are insensitive or slow to respond to epidermal growth factors following Nup153 knockdown. Likewise, in Drosophila, many instances of promoter-enhancer looping require Nup98 (Pascual-Garcia, Jeong and Capelson, Nucleoporin Nup98 associates with Trx/MLL and NSL histone-modifying complexes and regulates Hox gene expression 2014). Improper localization of repressor Nups during oncogene-induced senescence results in senescence-associated heterochromatin foci (SAHF), a hallmark sign of cancer cell nuclei. Knockdown of TPR, a human

Nup, partially relieves this SAHF phenotype in cancer cell lines, indicating a general role in heterochromatin formation during oncogenesis (Boumendil, et al. 2019).

THE NPC AS A TRANSCRIPTION ACTIVATOR

Interactions between chromatin and the NPC also have the potential to activate transcription. In budding yeast, genome-wide chromatin immunoprecipitation studies have shown hundreds of transcriptionally active loci interact with Nups (Casolari, Brown and Komili, et al. 2004, Casolari, Brown and Drubin, et al. 2005) and inducible genes reposition from the nucleoplasm to the nuclear periphery upon activation (Brickner and Walter 2004, Casolari, Brown and Komili, et al. 2004). In flies and mammals, thousands of chromosomal sites, including many euchromatic, transcriptionally active regions, interact with nuclear pore proteins (Brown, et al. 2008, Capelson, et al. 2010, Kalverda 2010, Liang, et al. 2013, Jacinto 2015, Pascual-Garcia, Debo, et al. 2017). These interactions enhance transcription and increase the rate of expression; disrupting the interaction with nuclear pore proteins reduces the rate and extent of transcriptional induction of many genes in budding yeast and animals (Brickner, Cajigas, et al. 2007, Ahmed, et al. 2010, Capelson, et al. 2010, Light, Brickner, et al. 2010, Liang, et al. 2013, Jacinto 2015). However, tethering inducible genes to the nuclear envelope or the NPC does not cause transcriptional activation, suggesting that physical proximity to the nuclear periphery is insufficient for impacting an individual gene's expression (Brickner and Walter 2004, Ahmed, et al. 2010, Green, et al. 2012, Texari, et al. 2013).

How do Nups promote transcription? Single-molecule RNA FISH experiments suggest that disrupting the interaction with the yeast NPC only reduces the fraction of cells within a population expressing induced genes, such as *GAL1* (Brickner, Sood, et al. 2016). The physical recruitment to the NPC requires a chromosomal locus to interact with specific transcription factors, also referred to as "positioning factors," via binding sites typically within their promoter that are called "zip codes." Preventing NPC interaction through mutating a positioning factor or zip code reduces the frequency and duration of transcriptional bursts, but the transcription rate, or ‘‘amplitude,’’ is mainly unaffected (Rodriguez and Larson 2020). This observation suggests that interaction with Nups quantitatively increases transcription burst

frequency and the duration of transcriptional activity without affecting the actual rate of RNA synthesis. Because proximal enhancers are implicated in burst frequency, while core promoter strength primarily affects burst amplitude (Tunnacliffe, Corrigan and Chubb 2018, Larsson, et al. 2019), this suggests that Nups stimulate enhancer function as a means to regulate expression.

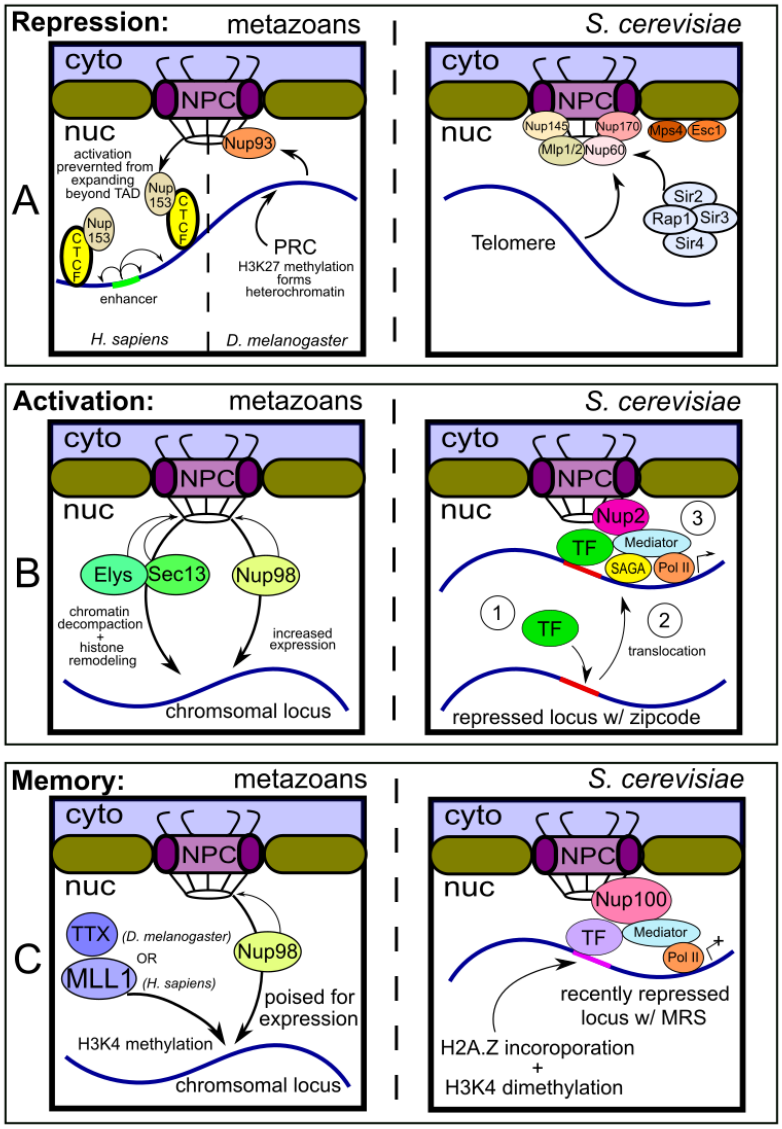

Figure 1.2 Nuclear pore complex (NPC) proteins affect transcription. (A–C) Schematic of metazoan nucleus (left) or yeast nucleus (right). (A) Nup-mediated transcriptional repression. (Left) Soluble Nup153 interacts with CTCF at topologically associated domain (TAD) boundaries in *Homo sapiens*. Heterochromatin at the nuclear periphery interacts with Nup93 and maintains Polycomb repressive complex (PRC) histone modification in *Drosophila melanogaster*. (Right) Telomere recruitment to the *Saccharomyces cerevisiae* NPC facilitates binding of chromatin silencing Sir factors. (B) Nup-mediated transcriptional activation. (Left) Chromatin decompaction by recruitment of Nups and transcriptional activation by recruitment of Nup98. (Right) Transcription factor (TF)- and Nup-dependent stimulation of transcription in *S. cerevisiae*. (C) Nup-dependent transcriptional poising. (Left) Nup98 recruitment can both enhance promoter–enhancer looping and, potentially, through recruitment of specific histone methyltransferases. (Right) Schematic of a Nup100-dependent chromatin changes leading to transcriptional poising during memory in *S. cerevisiae*. (MRS) Memory recruitment sequence.

An additional hint into the role of yeast Nups in transcriptional activation comes from structure-function analysis of the Gcn4 transcription factor. Gcn4 is essential for both transcriptional activation and NPC interaction of many target genes (Hope and Struhl 1985, Rawal, et al. 2018, Brickner, Randise-Hinchliff, et al. 2019, Randise-Hinchliff, et al. 2016). Tethering Gcn4 to a nucleoplasmic locus is sufficient to target that locus to the nuclear periphery, allowing identification of a minimal portion of Gcn4 necessary and sufficient to promote interaction with Nups. This strategy identified a positioning domain within the Gcn4 transcription factor (PDGCN4), a 27 amino acid peptide, separable from the activation domains. Mutation of three amino acids within this sequence disrupts the interaction of Gcn4 target genes with the NPC and results in a global defect in transcriptional activation of Gcn4 target genes (Brickner, Randise-Hinchliff, et al. 2019). Tethering of the PDGCN4 to an ectopic locus led to interaction with Nup2, but not with coactivators like SAGA or Mediator. These results argue that Nup interaction can stimulate activator domain-dependent transcription but cannot activate transcription without an activator domain.

In yeast, zip code-mediated targeting to the nuclear periphery also leads to inter-chromosomal clustering of genes that share the same zip codes (Brickner, Ahmed, et al. 2012). For example, upon inositol starvation, the two alleles of *INO1* reposition to the nuclear periphery and cluster. This requires the zip codes, the TFs that bind to the zip codes, and nuclear pore proteins. In haploid cells, inter chromosomal clustering can be observed by comparing the position of two loci that are targeted to the nuclear periphery by the same zip code. For example, active *INO1* clusters with both *URA3:GRS1* and another GRS I–containing gene, *TSA2*. Upon inositol starvation, the distribution of distances between alleles of *INO1* shifts to significantly shorter distances which is dependent on the upstream recognition sequence (URS) which contains the GRS sequences (Fig. 1.3 B, C).

Metazoan Nups are also known to induce activation when interacting with chromatin (Fig. 1.2 B). Knockdown of Nups in flies leads to a widespread decrease in transcription (Capelson, et al. 2010). Likewise, loss of Nup98 in embryonic stem cells impacts transcription and developmental potential (Liang, et al. 2013) and loss of the tissue specific Nup210 inhibits proper muscle cell gene expression and differentiation (D'Angelo, et al. 2012, Raices, et al. 2017). Although Nups interact throughout the genome, they bind strongly at super-enhancers (Ibarra, et al. 2016). These effects correlate with impacts on chromatin folding and structure. Interaction with Nups facilitates the recruitment of cohesin and the

formation of topologically associated domains (TADs) and promoter–enhancer looping (Pascual-Garcia, Debo, et al. 2017, Kadota, et al. 2020). Tethering of Nups such as Sec13 or Elys recruits PBAP/Brm and GAGA to polytene chromosomes in Drosophila leads to ectopic chromatin decondensation (Fig. 1.2 B) (Kuhn, et al. 2019). Thus, the role of Nups in animals in promoting transcription may primarily relate to their roles in affecting chromatin folding and condensation.

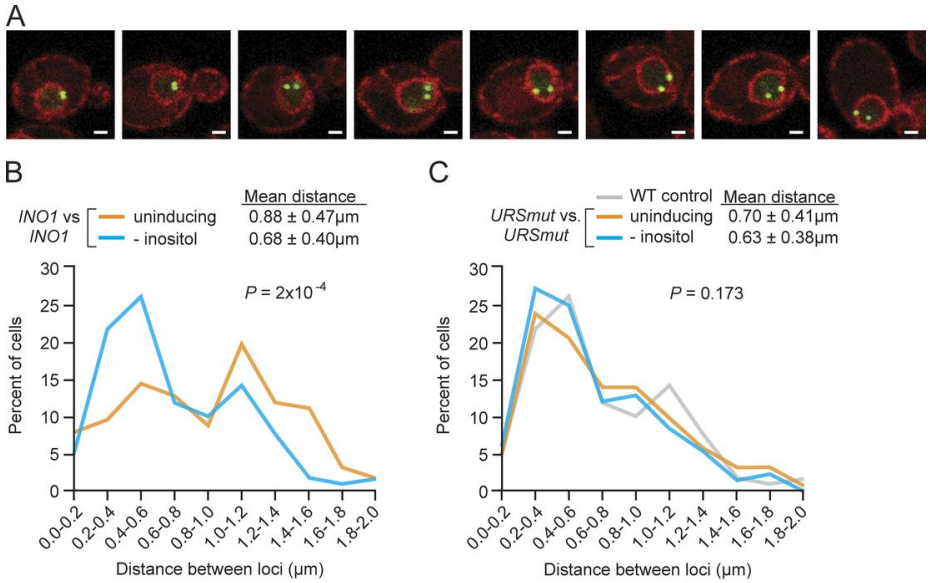

Figure 1.3 Transcription-associated peripheral localization leads to inter-chromosomal clustering in yeast. (A) Confocal micrographs of diploid cells having LacO arrays at each allele of *INO1,* expressing GFP-LacI and mCherry-ER marker. (B–D) Distances between *INO1* alleles were measured and binned into 0.2-µm bins, and the distribution of distances within the population was compared. In B and C, the p-value is from a Wilcoxon rank sum test comparing the distributions. In panel C, the gray line (wild-type [WT] control) is the distribution from B under the inducing condition.

Within plant nuclei, direct tethering of Nups to chromatin can modulate transcription. In *Arabidopsis thaliana*, binding the Nup Seh1 to a reporter transgene caused the chromatin to become localized at the nuclear periphery and stimulated transcription at the locus (Smith, et al. 2015). Likewise, Arabidopsis Nup1 is necessary for pollen and ovule development, and loss of Nup1 leads to a significant decrease in the expression of gametogenesis genes. It remains unclear whether these results are due to general NPC defects or changes in the capacity for genes to physically interact with the NPC. Additionally, the chlorophyll a/b gene locus undergoes light-dependent repositioning from the nuclear interior to the nuclear periphery upon transcriptional activation in certain species and cell types (Feng, et al. 2014). However, more exploration is required to determine a connection between plant cell transcription and the NPC.

THE NPC AS AN EPIGENETIC MEMORY REGULATOR

So far, this introduction has discussed how Nups interact with both active and silent loci and can both promote or repress transcription. However, Nups also play a conserved role in epigenetic transcriptional poising following specific stimuli and expression states. For example, when the yeast *INO1* locus becomes active, it is targeted to the NPC while in the active transcription state and remains targeted for multiple hours in both mother and daughter cells after it becomes repressed (Brickner et al. 2007). Despite the organizational effect being apparently identical, the molecular mechanism for targeting active *INO1* and recently repressed *INO1* utilize entirely different transcription factor and Nup components (Fig. 1.2 C) (Light, Brickner, et al. 2010). Whereas active *INO1* is targeted to the NPC by the gene recruitment sequences GRS I and GRS II and the transcription factors Put3 and Cbf1, recently repressed *INO1* is targeted to the NPC by the memory recruitment sequence (MRS), which binds the Sfl1 transcription factor. Furthermore, memory requires specific histone modifications and Nup100, while active *INO1* localization does not require either (D'Urso, et al. 2016). Thus, at least two separate mechanisms exist to target gene loci to the nuclear periphery for interaction with the NPC.

Transcriptional memory leads to changes in the chromatin state of the promoter, allowing the recruitment of a poised form of RNA polymerase II preinitiation complex (RNAPII PIC). This poised state of the promoter is activated more rapidly compared to the long-term repressed state. Poising provides an adaptive fitness advantage to recently repressed cells and their progeny. For the *INO1* gene, the loss of Sfl1, the MRS, or Nup100 blocks memory and results in activation more similar to the long-term repressed state.

The yeast transcriptional memory phenomenon is widespread and not just limited to the well-studied *INO1* locus. In yeast, many genes exhibit an enhanced activation rate if previously expressed, enhancing adaptive fitness (Sood, et al. 2017). Furthermore, memory is generally associated with specific changes in histone occupancy and modifications (H2A.Z incorporation, H3-lysine-4-dimethylation [H3K4me2]) and recruitment of a poised RNA polymerase II that remains within the pre-initiation complex (Fig. 1.2 C) (D'Urso, et al. 2016, Sood, et al. 2017). In this way, the NPC modulates potential future gene expression through a Nup100-dependent epigenetic mechanism on localized chromatin.

Metazoan cells also display Nup-dependent memory phenomena. In HeLa cells, interferon γ induced genes (IFN-γ) interact with Nup98 (the Nup100 homolog) upon removal of IFN-γ and continue this interaction for >4 days. These interferon response genes show faster/more robust expression upon second exposure to IFN-γ. Promoters of such poised genes are marked with H3K4me2 and bind RNA polymerase II. Transient knockdown of Nup98 during memory leads to a loss of H3K4me2 and RNA polymerase II from promoters and disrupts the faster reactivation rate. This establishes an ancient, conserved role for Nups in epigenetic transcriptional regulation (Light, Freaney, et al. 2013).

In flies, ecdysone-induced genes also interact with Nup98 and exhibit transcriptional memory. Brief exposure of S2 cells to ecdysone leads to Nup98 binding and poises target genes for induction (Pascual-Garcia, Debo, et al. 2017). The knockdown of Nup98 specifically disrupts this effect, leading to no memory. The effect of Nup98 in this system (and perhaps others) is to stabilize a promoter–enhancer loop. This loop is strengthened by previous treatment with ecdysone and by binding to Nup98, suggesting that Nup98-dependent chromatin folding can facilitate the establishment and inheritance of epigenetic states.

The effects of Nups on chromatin and transcription also has significant impact on human health. Chromosomal translocations that lead to translational fusions of Nup98 with several proteins such as HOXA9, HOXD13, Top1, and Nsd1 are known to lead to acute myeloid leukemia (AML) (Franks, et al. 2017). Why? Nup98 is associated with H3K4 methylation in flies and humans and interacts with the H3K4 methyltransferases Trithorax and MLL1, respectively (Fig. 1.2 C) (Kaltenbach, et al. 2010, Gough, Slape and Aplan 2011). These results led to the hypothesis that AML is due to excessive H3K4 methylation of target genes induced by ectopic recruitment of Nup98 at those loci. Indeed, the Nup98-Nsd1 fusion protein expressed in myeloid cells from AML patients binds to Wdr82, a component of the H3K4 methyltransferase Set1A/B-COMPASS. Forming this aberrant complex results in transcription-associated histone modifications at Nsd1 target genes, such as the *HOXA* locus, leading to an increase in expression (Michmerhuizen, Klco and Mullighan 2020). These findings show the critical role of Nup98/Nup100 in epigenetic regulation for both adaptive survival and pathogenic transcription.

In addition to mediating nucleocytoplasmic trafficking, the role of nuclear pore proteins in regulating transcription and chromatin structure is now more widely appreciated in the past few decades. Specific interactions between chromatin and Nups are associated with changes in spatial organization,

transcriptional silencing, transcriptional activation, transcriptional poising, changes in chromatin modifications, and changes in chromatin folding.

While epigenetics researchers are still exploring the precise molecular nature and mechanisms of these many roles, it is clear that the NPC is integral to regulating genome organization and gene expression. Moreover, quantifying parameters of gene movement in different organization states, such the diffusive velocity and degree of positional confinement, will help guide future hypothesis design and deepen the collective understanding of dynamic genome organization. With the ubiquity of the NPC amongst eukaryotes, studying how nuclear architecture interaction controls dynamic genome organization can uncover previously unknown methods of expression regulation. This has the implication of forming new detection methods for genome-related disease in patient derived tissues and tools for industrial strain engineering that may require an orthogonal approach to regulating transcriptional bursting. The relationship between NPC and genome organization is likely as old as the nucleus itself, but we are only beginning to appreciate the depth and complexity of regulatory mechanisms that have evolved between them since. The work in this thesis seeks to explain a mechanism in yeast for establishing and maintaining dynamic gene organization and help direct future work seeking to model similar emergent properties and quantifiable phenomena from large particle tracking data sets.

CHAPTER 2

TRANSCRIPTION-ASSOCIATED PERIPHERAL LOCALIZATION IN YEAST

Portions of this chapter were published in:

Randise-Hinchliff, C, R Coukos, V Sood, MC Sumner, S Zdraljevic,, L Meldi Sholl, DG Brickner, S Ahmed, L Watchmaker, & JH Brickner (2016). Strategies to regulate transcription factor-mediated gene positioning and interchromosomal clustering at the nuclear periphery. The Journal of cell biology, 212(6), 633–646. doi:10.1083/jcb.201508068

And

Sumner, MC, SB Torrisi, DG Brickner, & JH Brickner (2021). Random sub-diffusion and capture of genes by the nuclear pore reduces dynamics and coordinates inter-chromosomal movement. eLife, 10, e66238. doi:10.7554/eLife.66238

DETERMINING ROLE OF TFs, ZIP CODES, AND SAGA IN GENE LOCALIZATION

As discussed in the introduction, targeting inducible genes to the nuclear periphery in yeast is mediated by cis-acting transcription factor binding sites that function as DNA "zip codes" (Ahmed, et al. 2010). We sought to test whether other genes in yeast, the inducible genes *PRM1* (a cell surface transmembrane protein induced by mating pheromone) and *HIS4* (a multifunctional histidine biosynthetic enzyme induced by histidine starvation) undergo recruitment to the nuclear periphery in a transcription factor-dependent fashion similar to *INO1. PRM1* is among a set of genes previously shown to physically interact with the NPC when cells are in the presence of yeast mating pheromone peptide known as "alpha-factor". *HIS4* was identified as a putative NPC-interacting gene in silico comparison by comparing its promoter to other known NPC-interacting genes (Casolari, Brown and Komili, et al. 2004). Each in a different strain, an array of 128 Lac repressor binding sites was inserted downstream of *HIS4, PRM1, INO1,* and *URA3* (serving here as a nucleoplasmic control). These strains also express GFP-tagged Lac repressor (GFP-LacI) and an mCherry ER/nuclear envelope marker. The fraction of the cells in which the GFP-LacI focus colocalized with the nuclear envelope was quantified for inducing and repressing conditions. For all the observed genes, repressing conditions were nearly identical. However, the inducing conditions for each

respective gene increased the fraction of peripheral localization, except for the *URA3* control, which did not significantly change localization percentage regardless of inositol/amino acid starvation or pheromone exposure.

INO1, PRM1, and *HIS4* transcription-associated localization to the nuclear periphery requires specific transcription factors binding within their promoters. Targeting *INO1* to the nuclear periphery requires at least one of two cis-acting DNA elements, known as GRS I and GRS II (Ahmed et al., 2010). The Put3 transcription factor binds to the GRS I zip code and is necessary for GRS I–dependent localization. The transcription factor Cbf1 acts similarly with the GRS II zip code (Brickner, Ahmed, et al. 2012, Ahmed, et al. 2010). Neither zip code/TF pair is dependent on the other, giving *INO1* a unique backup method for maintaining localization. The positioning of *PRM1* and *HIS4* to the nuclear periphery requires the same TFs that regulate their expression. Cooperative binding of the Ste12 TF to three pheromone response elements (PREs) within the *PRM1* promoter serves as a zip code and regulates its transcription. Loss of Ste12 blocks *PRM1* localization to the nuclear periphery while in the presence of mating pheromone. *HIS4* expression requires binding of the Gcn4 TF to binding sites within the promoter region (Arndt and Fink 1986), and loss of Gcn4 blocks positioning of *HIS4* (and other histidine starvation response genes) to the nuclear periphery. Therefore, the subnuclear positioning of *INO1, PRM1*, and *HIS4* each require specific transcription factors binding to their zip code-bearing promoters.

The SAGA histone acetyltransferase complex is necessary to recruit genes such as *GAL1-10* and *INO1* to the NPC (Rodríguez-Navarro, et al. 2004, Luthra, et al. 2007, Ahmed, et al. 2010, Strambio-De-Castillia, Niepel and Rout 2010). In order to test whether *HIS4* and *PRM1* recruitment to the NPC requires SAGA, a component of SAGA necessary for the complex's structural integrity and function, known as Spt20 (Roberts and Winston 1997) was knocked out of the previously mentioned microscopy strains. Loss of Spt20 blocked recruitment of both *INO1* and *HIS4* to the nuclear periphery (Fig. 2.1 B). However, *PRM1* repositioning to the nuclear periphery was independent of Spt20. Thus, peripheral recruitment of some genes, but not all, appears dependent on SAGA structure or function. To address whether transcription is necessary for peripheral localization, it became imperative to test whether a transcription factor binding site could mediate peripheral localization when inserted at an ectopic locus. Binding sites were inserted proximal to the *URA3* locus to test its sufficiency to promote peripheral localization (Ahmed, et al. 2010).

Both GRS I and GRS II are sufficient to reposition *URA3* to the nuclear periphery (Fig. 2.1 C). Put3 was required for GRS I–mediated gene positioning, Cbf1 was required for GRS II–mediated gene positioning, and SAGA was required for both. Insertion of three PREs (3×PRE) or the Gcn4 binding site at *URA3* was also sufficient to promote peripheral localization under endogenous induction conditions, and these zip codes required Ste12 and Gcn4, respectively (Fig. 2.1 D).

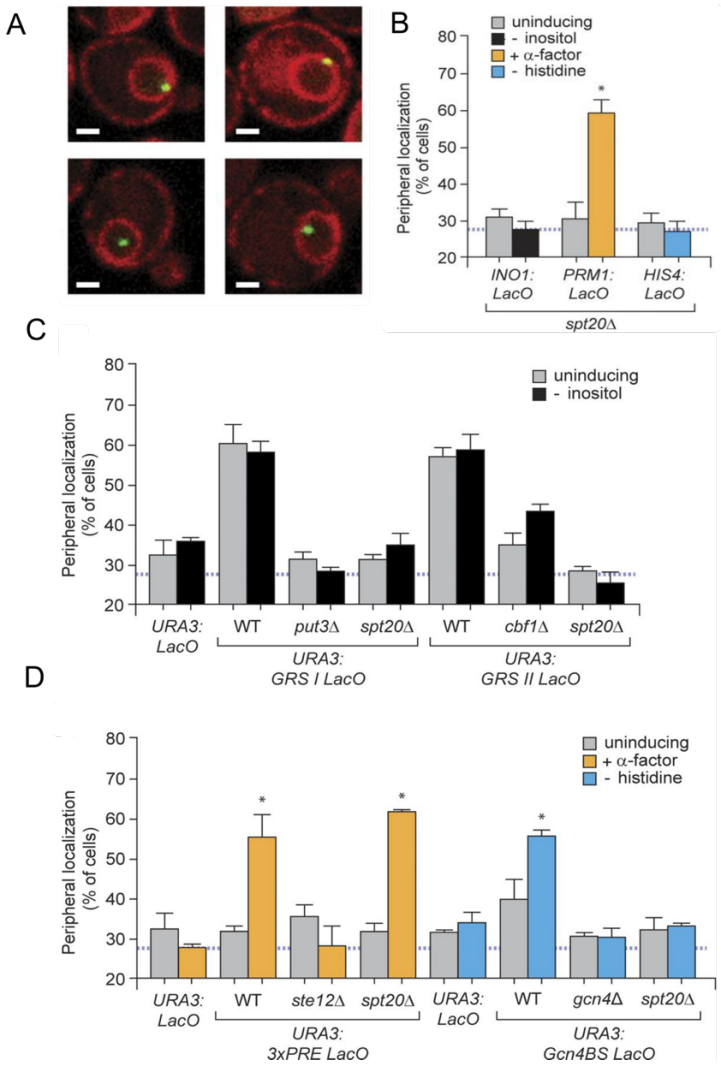

Figure 2.1 Transcription factor binding sites function as DNA zip codes, and most are dependent on SAGA function. (A) Fluorescence micrographs of green LacO/LacI array and red membrane marker. Top row classified as peripheral, bottom as nucleoplasmic. (B) Peripheral localization of endogenous loci in *SPT20* knockouts (C and D) Peripheral localization of the *URA3* locus, ± indicated DNA BSs, grown under uninducing and inducing conditions. GRS I or GRS II (C), 3×PREs (D), or Gcn4 BS (D) were inserted at *URA3* in wild-type (WT) and mutant strains. *, P ≤ 0.05 (Fisher exact test) comparing uninducing and inducing condition. Mean and SEM from three of more biological replicates (30–50 cells per replicate)

It is important to highlight that the time required for different stimuli to cause peripheral localization, and by extension clustering, varies depending on the method of regulation (Fig. 2.2 A-C). But are the disparate time scales due to differences in the positioning mechanism (sub- vs. super-diffusion) or purely due to differences in TF expression and regulation (Fig 2.2 D). To answer this, the movement of genes within the nucleoplasm and positioned at the periphery must be tracked and quantified. With this information, it will become much easier to identify movement that is unlike these two steady states and improve our fundamental understanding of gene movement within the nucleus.

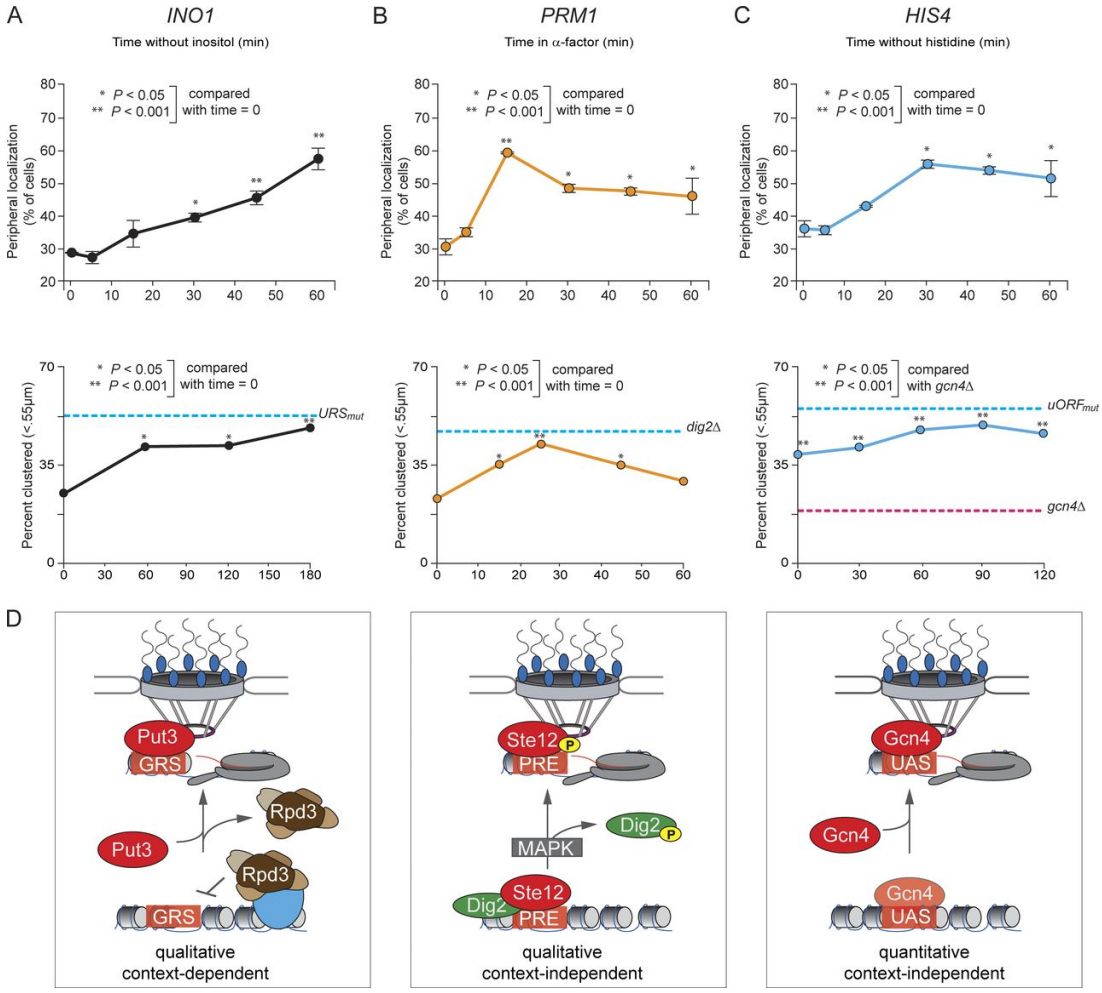

Figure 2.2 Different regulatory strategies lead to large-scale changes in nuclear organization over different time scales. (A–C) Time course after shifting to –inositol (A), +α-factor (B), or –histidine (C). (top) Peripheral localization of *INO1* (A), *PRM1* (B), and *HIS4* (C). (bottom) Percentage of cells in which the two loci were ≤0.55 μm for *INO1* versus *INO1* in diploid cells (A), *PRM1* versus *URA3:3×PRE* in haploid *MAT***a** cells (B), and *HIS4* versus *HIS4* in diploid cells. (D) Schematic for three distinct mechanisms of regulation of gene positioning. *, P ≤ 0.05; **, P ≤ 0.001 (Fisher exact test) between SDC and inducing condition.

NUCLEOPLASMIC OR PERIPHERAL: DIFFERENCES IN DIFFUSIVE MOVEMENT

In static confocal microscopy experiments, repositioning of inducible genes such as *HIS4* or *INO1* to the periphery leads to an increase in the fraction of cells in which the locus colocalizes with the nuclear envelope from that expected for a random distribution (~30%) to ~50–65% (Fig. 2.3 B, D) (Brickner and Walter 2004, Egecioglu, et al. 2014). However, artificially tethering chromatin to the nuclear envelope leads to ~85% colocalization with the nuclear envelope (Brickner and Walter 2004). This suggests that localization to the nuclear periphery reflects either dynamic or continuous interaction with the NPC or two distinct populations of cells, one that exhibits stable association with the nuclear envelope and the other that does not. To distinguish between these possibilities, we quantified peripheral localization of three LacO-tagged loci over time in individual cells: the inducible genes *HIS4* and *INO1*, as well as the negative control *URA3*, which localizes in the nucleoplasm (Fig. 2.3 B, D) (Brickner, Randise-Hinchliff, et al. 2019, Randise-Hinchliff, et al. 2016). To avoid the complication that interaction of many genes with the NPC is lost during S-phase, cells were synchronized using nocodazole and released into G1 for 30 min before scoring colocalization with the nuclear envelope every 10 s over 10 min (Brickner and Brickner 2010). In complete media (i.e., uninducing conditions), all three genes showed similar patterns: episodic, brief colocalization with the nuclear envelope (Fig. 2.3 C, E, and F). However, under inducing conditions (histidine for *HIS4* or inositol for *INO1*), the pattern changed. Both *HIS4* and *INO1* showed longer periods of colocalization with the nuclear envelope (Fig. 2.3 C, F, and J), while *URA3* was unaffected (Fig. 2.3 E). The pattern was consistent across the population so that the fraction of cells in which *HIS4* or *INO1* colocalized with the nuclear envelope at each time point (Fig. 2.3 H) was in close agreement with the fraction of time spent colocalized with the nuclear envelope in each cell (Fig. 2.3 I). This argues against two distinct populations and instead suggests that interaction with the NPC is continuous and dynamic over time, increasing the duration of colocalization with the nuclear envelope.

Interaction with the NPC is mediated by transcription factors binding to cis-acting elements that function as DNA zip codes (Ahmed, et al. 2010, Brickner, Randise-Hinchliff, et al. 2019, Light, Brickner, et al. 2010). For example, the Gene Recruitment Sequence GRS I from the INO1 promoter binds to the Put3 TF to mediate interaction with the NPC and positioning at the nuclear periphery (Brickner, Ahmed, et al.

2012). Likewise, the Gcn4 binding site (GCN4 BS) from the *HIS4* promoter is sufficient to mediate interaction with the NPC (Randise-Hinchliff, et al. 2016). Inserting zip codes near *URA3* is sufficient to reposition *URA3* to the nuclear periphery (e.g., *URA3:GRS1*, Fig. 2.3 D) (Ahmed, et al. 2010, Randise-Hinchliff, et al. 2016). The association of *URA3:GRS1*, which shows unregulated localization to the periphery, with the nuclear envelope over time resembled that of active *HIS4* and *INO1* (Fig. 2.3 G–J). Thus, DNA zip code-mediated interaction with the NPC is sufficient to produce continuous and dynamic association with the nuclear envelope.

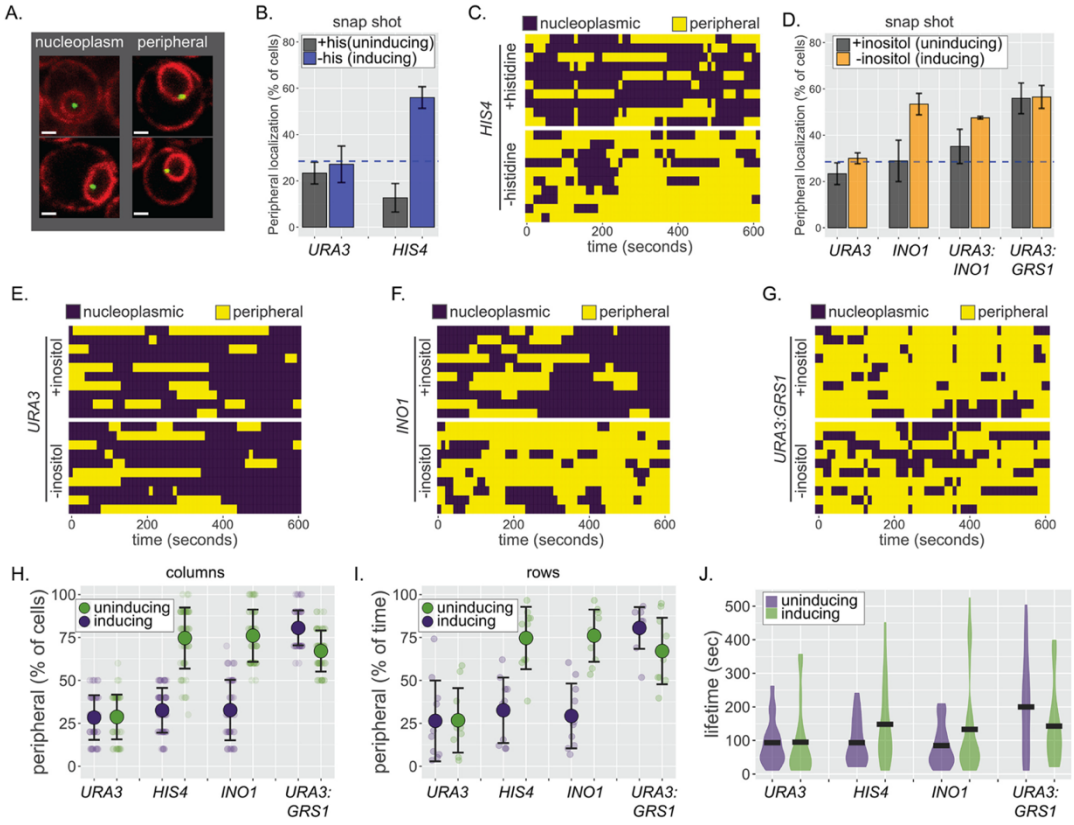

Figure 2.3 Continuous and dynamic positioning at the nuclear periphery. (A) Representative confocal micrographs of cells having the LacO array integrated at a locus of interest, expressing GFP-LacI and Pho88-mCherry and scored as either nucleoplasmic (left) or peripheral (right). (B) Peripheral localization (% of cells ± SEM) of *URA3* and *HIS4* in cells grown ± histidine. The hatched blue line, here and throughout: peripheral localization predicted by chance. (C, E–G) Kymographs of 10 cells with a LacO array integrated at *HIS4* (C), *URA*3 (E), *INO1* (F), or *URA3:GRS1* (G) were grown in the indicated medium and scored for peripheral localization every 10 s for 5 min. Yellow: peripheral; purple: nucleoplasmic. (D) Peripheral localization (± SEM) of *URA3*, *INO1*, *URA3:INO1*, and *URA3:GRS1* in cells grown ± inositol. (H– J) Summary plots from (C, E–G): (H) mean percentage of cells (± SD) in which the locus is peripheral at each time point (i.e., each dot represents a summary of a single column from kymographs); (I) mean percentage of time (± SD) each locus spent colocalized with the nuclear envelope (i.e., each dot represents a summary of a single row from kymographs); and (J) the distribution and median duration of periods of peripheral localization of each locus.

We next examined how interaction of genes with the NPC impacts the dynamics of diffusion using MSD analysis. MSD has been used to show that chromosomal loci exhibit constrained sub-diffusion (Marshall, et al. 1997). For comparison, we tracked the movement of the less-mobile nuclear envelope-embedded spindle pole body (SPB) and a much more mobile cytoplasmic particle (the μNS viral capsid; Munder et al., 2016). While μNS was highly diffusive, the SPB showed very limited displacement at this timescale, reflecting both slow diffusion within the membrane and movement of the whole nucleus (Fig. 2.4 B). The MSD of 11 nucleoplasmic loci (i.e., not associated with the NPC) and two telomeres tethered to the nuclear envelope exhibited a range of intermediate sub-diffusion between these two extremes, with the nucleoplasmic loci showing greater MSD than tethered telomeres and telomeres showing greater MSD than the SPB (Fig. 2.4 B). Simultaneously acquiring images of chromosomal loci and the SPB to correct for nuclear movement significantly reduced the time resolution (data not shown). Given that nuclear movement was much less than chromosomal movement at these timescales, it could be ignored. We also determined the MSD of chromosomal loci in 3D. Although this gave very similar results, the quality of the data was lower because of the longer time interval (>1 s). For these reasons, we limited our movies for MSD analysis to 40 s at 210 ms resolution (200 0.21 s) in a single focal plane and calculated MSD for time intervals between 210 ms and 4 s (Fig. 2.4 B).

The nucleoplasmic loci showed a range of mobility by MSD, perhaps reflecting nearby physical interactions with the nuclear envelope. Tethering to the nuclear envelope has a significant effect on chromatin positioning and diffusive range (Avşaroğlu, et al. 2014, Verdaasdonk, et al. 2013). Indeed, the initial MSDs (t = 0.21 s) showed a non-linear relationship to the genomic distance to the nearest nuclear envelope tethering point (either centromeres or telomeres; Fig. 2.4 C). Consistent with work from others, we could model this relationship as a hyperbolic curve with a half-maximal MSD observed at ~18 kb (Fig. 2.4 C, blue dashed line) (Avşaroğlu, et al. 2014, Verdaasdonk, et al. 2013). Thus, chromatin diffusion is influenced over relatively short distances by stable interactions with the nuclear envelope (Hediger, Neumann, et al. 2002, Hediger, Berthiau, et al. 2006). To quantify the effect of local interaction with the NPC on chromatin sub-diffusion, we examined genes that show conditional association with the NPC. We compared the MSD of *INO1*, *HIS4*, and *URA3* under either uninducing or inducing conditions (±histidine and ±inositol). As expected, *URA3* showed no change in MSD under these conditions (Fig. 2.4 D). However,

both *HIS4* and *INO1* showed significantly reduced mobility upon induction (Fig. 2.4 E, F), confirming that repositioning to the nuclear periphery correlates with reduced chromatin sub-diffusion.

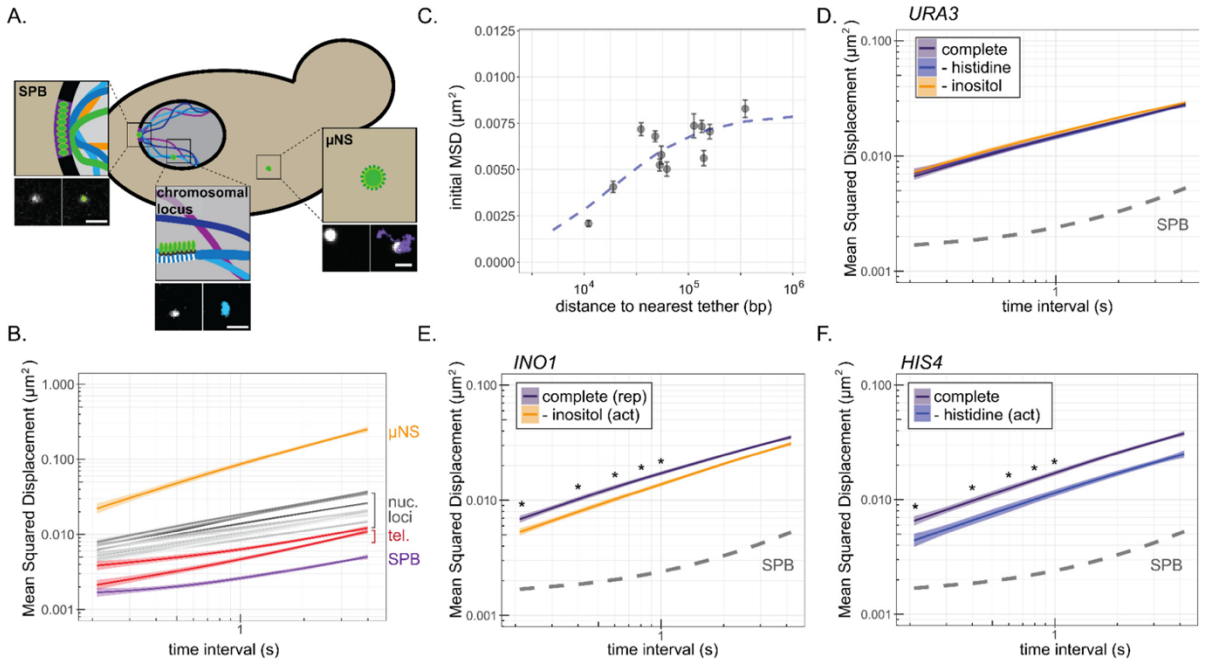

Figure 2.4 Mean-squared displacement (MSD) of chromatin sub-diffusion. (A) Schematic of fluorescent foci within the yeast cell. Fluorescently tagged spindle pole body (SPB), cytoplasmic μNS, and chromosomal locus were tracked over 200 200 ms. Example micrographs of each particle (left) and overlaid path (right) are shown for each. Scale bar = 1 μm. (B) Average MSD for μNS (orange), SPB (purple), 10 nucleoplasmic loci (gray) and two telomeres (red) at different time intervals (t). The ribbon around the mean represents standard error. (C) Mean MSD ± standard deviation for t = 200 ms for each chromosomal locus in (B) vs $\log_{10}$ (base pairs) to the nearest tether point (centromere or telomere). The line is from the fit of the data to a non-linear model for a hyperbolic curve, as described in the text. (D–F) MSD plots of *URA3* (D), *INO1* (E), or *HIS4* (F) in cells grown in the indicated media. In all plots, the dashed line represents the MSD of the SPB. *p<0.05 based on Kolmogorov–Smirnov test comparing MSDs at the indicated times.

To further strengthen this correlation, we exploited the population dynamics illuminated in Figure 4, performing MSD analysis on sub-populations of cells in which the locus was either stably maintained at the nuclear periphery (i.e., those cells in which >50% of the time points were peripheral) or predominantly in the nucleoplasm (<10% peripheral) during the 40 s acquisition. When we performed this analysis with repressed *INO1*, the MSD from predominantly peripheral cells was indistinguishable from the MSD from predominantly nucleoplasmic cells. However, for active *INO1*, the MSD from predominantly peripheral cells was significantly lower than the MSD from predominantly nucleoplasmic cells, consistent with the decrease

in MSD resulting from interaction with the NPC (Figure 2.4). At this point there is still the possibility that the periphery imparts drag on proximal chromatin with a local, active gene, and it remains unclear whether the NPC is required for this reduction in movement to occur.

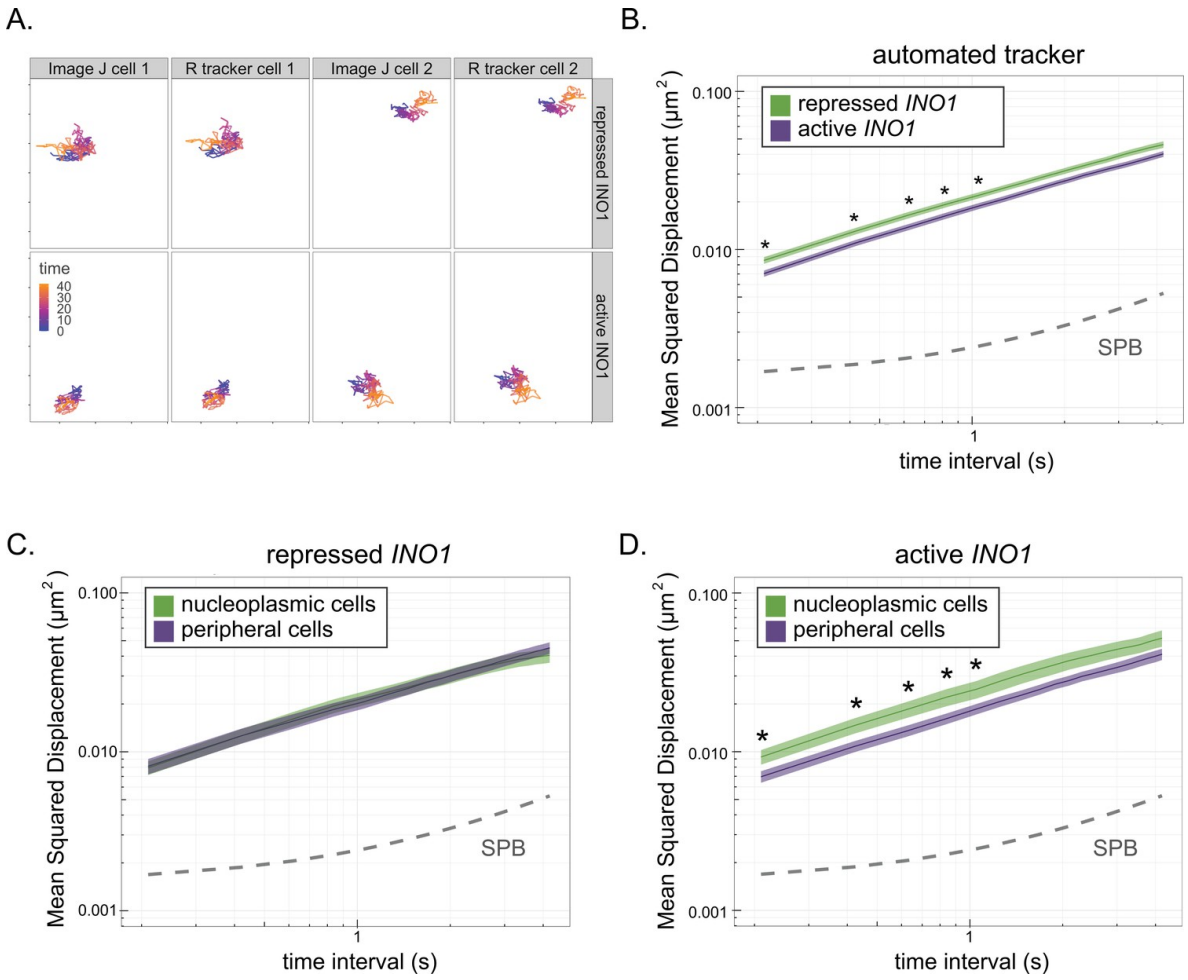

Figure 2.5 MSD of loci in cells that are predominantly peripheral or nucleoplamsic. To monitor peripheral localization during particle tracking for MSD, we developed an automated tracking system in R that uses the imageR package to threshold, denoise, and detect both the nuclear periphery and the center of mass of fluorescent loci. Markdowns containing the functions used in this system are available through GitHub (https://github.com/MCnu/R_sim_scripts) (**A**) Comparison of the Image J tracking method (see Materials and methods) to the R tracker. Repressed or active *INO1* were tracked in two representative cells over time with each method, and the resulting paths are shown. (**B**) MSD analysis of repressed and active *INO1* using the R tracker. (**C, D**) MSD analysis of repressed *INO1* (**C**) or active *INO1* (**D**) from cells in which the locus was predominantly nucleoplasmic or predominantly peripheral. For repressed *INO1*, the nucleoplasmic population (n = 22) had >90% nucleoplasmic steps, and the peripheral population (n = 22) showed >40% peripheral steps over 40 s. For active *INO1*, the nucleoplasmic population (n = 20) showed >75% nucleoplasmic steps and the peripheral population (n = 20) showed >60% peripheral steps over 40 s.

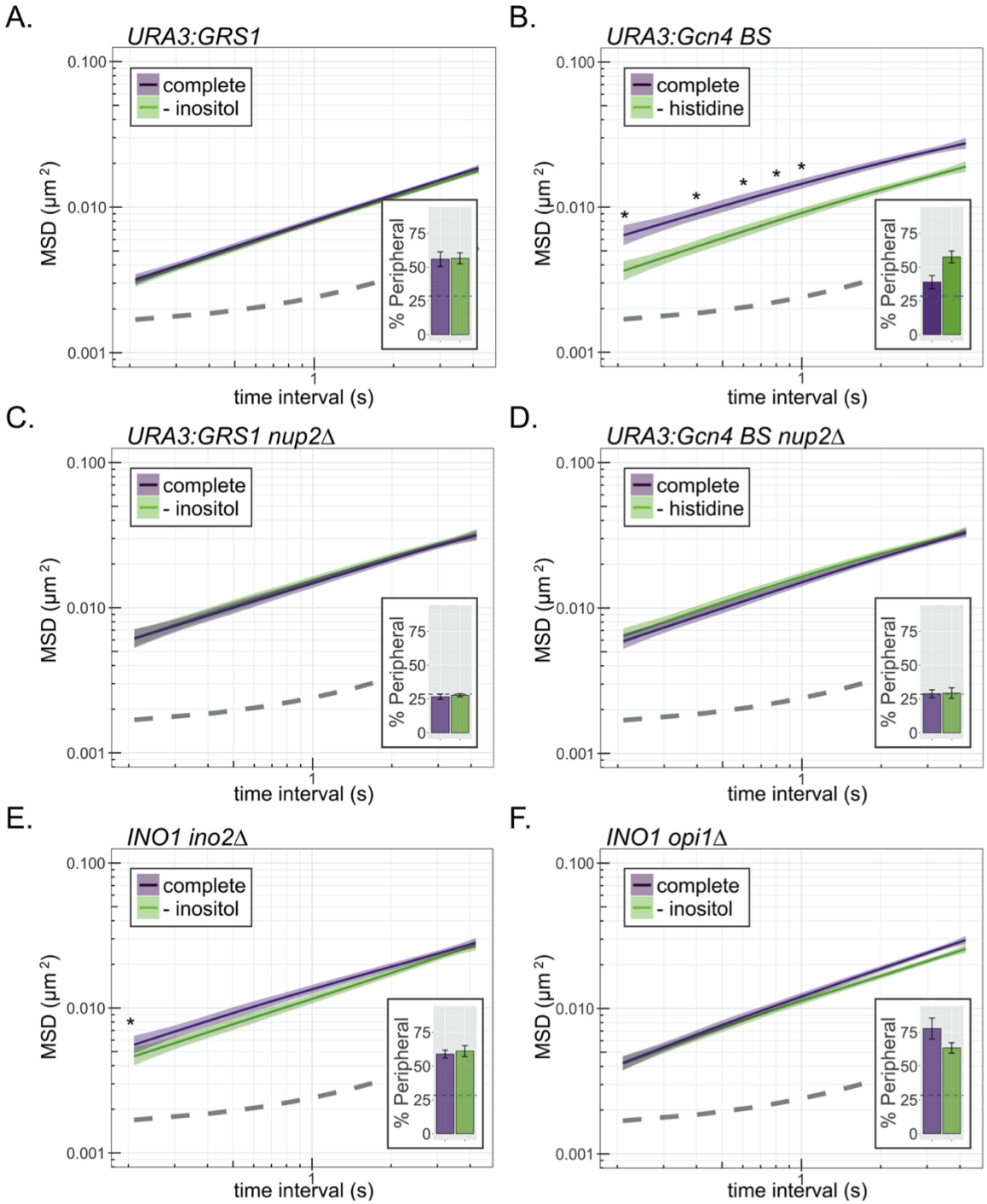

Figure 2.6 Interaction with the NPC reduces chromatin sub-diffusion. (A–F) MSD of *URA3* (A–D) and I*NO1* (E, F) in strains grown in the indicated media. Dark line indicates average MSD, ribbon = bootstrapped SEM. Insets: peripheral localization of each locus (mean % of cells ± SEM). The GRS I zip code from the I*NO1* promoter (A, C) or the Gcn4 binding site (B, D) was integrated and integrated at *URA3* in wild-type (A, B) or *nup2Δ* (C, D) strains. MSD of *INO1* in i*no2Δ* or *opi1Δ* (F) strains. *p<0.05 based on Kolmogorov–Smirnov test comparing MSD at the indicated time points.

If the change in MSD is due to interaction with the NPC, a DNA zip code integrated at an ectopic site should also reduce MSD. Single copies of zip codes from the promoters of *INO1* (*URA3:GRS1*; Fig. 2.5 A) or *HIS4* (*URA3:GCN4BS*; Fig. 2.5 B) were integrated at the *URA3* locus. *URA3:GRS1* localizes at the nuclear periphery constitutively (Fig. 2.1 D and 2.6 A) (Ahmed, et al. 2010) (Randise-Hinchliff, et al. 2016), resulting in a reduced MSD under all conditions. In contrast, *URA3:GCN4BS* shows conditional localization to the periphery upon amino acid starvation (Fig. 2.6 B, inset; Randise-Hinchliff et al., 2016), and a conditional reduction in MSD (Fig. 2.6 B). Loss of the NPC protein Nup2 disrupts DNA zip code-mediated localization to the nuclear periphery and resulted in MSD similar to *URA3* under all conditions (Fig. 2.6 C, D). Thus, DNA zip code-mediated interaction with the NPC is sufficient to suppress chromatin sub-diffusion.

To disentangle the effects of peripheral localization from the effects of transcriptional activity on MSD, we monitored MSD in mutants that lack trans-acting transcriptional regulators of the *INO1* gene. Both *INO1* transcription and *INO1* interaction with the NPC are regulated by the Opi1 repressor, which recruits the Rpd3L histone deacetylase to regulate binding of the Put3 transcription factor to the GRS I zip code (Randise-Hinchliff, et al. 2016). Because Opi1 is recruited to the *INO1* promoter by binding to the Ino2 activator (Heyken, et al. 2005), loss of either Ino2 or Opi1 leads to constitutive peripheral localization (Fig. 2.6 E, F, insets) (Randise-Hinchliff, et al. 2016). However, these two mutants have opposite effects on *INO1* transcription: *ino2Δ* blocks all expression, while *opi1*Δ shows unregulated, high-level expression. In both mutants, the *INO1* MSD resembled that of active *INO1* (Fig. 2.6 E, F), suggesting that interaction with the NPC is the principal cause of the decrease in sub-diffusion.

DISCUSSING CHROMATIN DIFFUSION CONFINEMENT

Previous work has shown that transcriptional activation and chromatin remodeling can cause increased chromatin mobility (Gasser, et al. 2004, Gu, et al. 2018). This could very well be the case for some active genes that are active and predominantly positioned in the nucleoplasm, though we observed contrary results (Fig. 2.5 D). There is still the possibility that movement could be increased for specific loci not assayed in this work. But shown in the prior section, the *INO1* locus movement was nearly

indistinguishable whether it was the active locus in wild-type or either the i*no2Δ* or *opi1Δ* backgrounds despite very different levels of transcription occurring at the same locus. In addition, active loci (*INO1:LacO / HIS4:LacO* in inducing conditions) in a *nup2Δ* background did not show significantly greater movement compared to wild-type backgrounds. That said, research looking into the periodicity of transcription bursts with oscillations between the periphery and nucleoplasm for active genes as in Fig. 2.3 C could help determine if transcription has a more direct role in the localization and movement of a gene locus. Methods for such experiments using a nascent transcript visualization system are detailed in the final chapter.

Taken together, our data shows that both endogenous and ectopic locus peripheral localization have a significant impact on diffusion rate. While the average velocity is less for induced peripheral loci, they remain mobile and periodically travel into the nucleoplasm (Fig. 2.3). The physical interactions that keep the locus at the periphery must be highly unstable but quickly re-established to damp chromatin movement in this way. This reduction in diffusive rate is dependent on Nup2 and likely other NPC components known to be required for peripheral localization. In addition, the reduction in diffusion was not dependent on the transcription state of the local chromatin. In fact, ectopic insertion of zip codes at *URA3* induced greater confinement than at the zip codes' endogenous site. With a better understanding of chromatin dynamics within the nucleoplasmic and peripheral states, tracking chromatin movement during transition between these states could provide data on the underlying translocation mechanism that establishes positioning.

With this expansive tracking data set, it was possible to devise multiple models that could replicate different features of our observed data. But a proper model capable of simulating gene diffusion trajectories using defined MSD, time parameters, and tunable boundary affinity is necessary to recapitulate and compare against our *in vivo* data. And to do so requires further exploration of the mechanics of chromatin dynamics within the nucleus, the forces affecting chromosome organization, and fundamental properties of diffusive movement.

CHAPTER 3

QUANTIFYING AND MODELING GENE MOVEMENT DURING TRANSLOCATION AND CLUSTERING

Portions of this chapter were published in:

Sumner, M. C., Torrisi, S. B., Brickner, D. G., & Brickner, J. H. (2021). Random sub-diffusion and capture of genes by the nuclear pore reduces dynamics and coordinates inter-chromosomal movement. eLife, 10, e66238. Doi:10.7554/eLife.66238

FRACTIONAL BROWNIAN MOTION AND INITIAL SIMULATIONS

The nucleus provides eukaryotic cells with a membrane-enclosed organelle that houses nearly all of its genome content and isolates that genome from the processes occurring in the cytoplasm. Though isolated, the nuclear compartment is still a chaotic environment with molecules constantly diffusing and colliding with each other and the nuclear envelope. As such, particles diffuse within the nucleus in a stochastic manner that is more confined than “perfect” diffusion, or Brownian motion. This reduced movement is commonly referred to as “Sub”-diffusion. We showed previously that there are differences in diffusion rate between genes localized in the nucleoplasm and at periphery, and that data can now be used to test against different modeling approaches to simulate gene movement.

$$\overline{D}^2 = \Gamma \times t^{\alpha}$$

Equation 3.1. Simplified MSD equation. Mean squared displacement is equivalent to the Diffusion Coefficient (Γ) multiplied by the interval of time over which diffusion occurred raised to the power that defines the type of diffusion (t^{α}). When α is between zero and one the movement is “sub-diffusive,” while α greater than one indicates “super-diffusion.”

Using parameters from the MSD analysis, we developed a simulation of chromatin sub-diffusion (https://github.com/MCnu/YGRW). Sub-diffusion of a segment of chromatin results from forces affecting the chromatin segment both directly (e.g., the viscoelastic potential of the polymer, boundary collision) and indirectly (forces and membrane tethering nearby). Chromatin sub-diffusion has been modeled using several approaches (Arbona, et al. 2017, Verdaasdonk, et al. 2013). Anticorrelated movement cannot be reproduced through either a random walk or a simple process of weighted step sizes derived from our experimental observations (Fig. 3.1). However, a continuous-time Gaussian process known as fractional

Brownian motion (FBM) produces trajectories that approximate chromatin sub-diffusion (Lucas, et al. 2014). FBM produces non-independent steps across time, allowing us to impart the anticorrelation between individual steps characteristic of yeast chromatin sub-diffusion. For each trajectory, two numeric arrays for the x and y dimensions of movement (Dietrich and Newsam, 1997) were generated based on an expected covariance matrix and α = 0.52 (Eq. 3.1). This array produces a stochastic time series of vectors with an anticorrelation structure functionally identical to that observed for chromatin movement. Finally, these vectors were scaled according to the experimentally derived G value and Hurst exponent (Mandelbrot and Ness 1968). Starting from random positions within the nucleus, the resulting array of discrete step lengths describes a single, two-dimensional sub-diffusive particle trajectory. This rapid and straightforward approach generates trajectories similar to our experimental observations and imparts memory resembling the MSD of chromosomal loci in the nucleoplasm (Fig. 3.1 A).

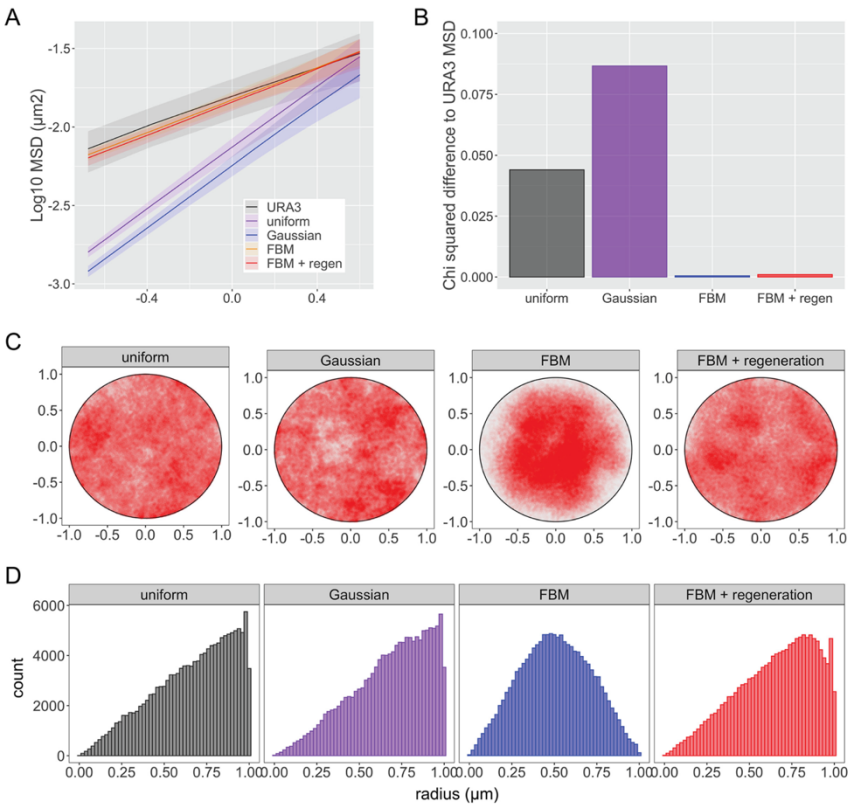

Figure 3.1 Comparison of simulations of sub-diffusion of nucleoplasmic chromatin. Four different simulations of chromatin diffusion were compared with *URA3* for MSD (A, B) or nuclear position (C, D). The uniform simulation generated uniformly distributed step sizes in the x and y dimensions with a mean step size of 0 ± 0.05 μm. The Gaussian simulation generated normally distributed step sizes in the x and y dimensions with a mean step size of 0 and a sigma of 0.025 μm. The fractional Brownian motion simulation (FBM) and a modified FBM with regeneration are detailed in Materials and methods (G = 0.015 $\mu m^2 s^{-1}$, a = 0.52). Each simulation condition consists of 100 trajectories, each composed of 2000 steps at 210 ms step time intervals. (A) Plot of MSD for *URA3* and the different simulations. (B) X^2 sum of differences between mean MSD plots of *URA3* and each simulation (t = 4 s). (C) Positions generated over 5 min of 100 simulations for each type. (D) Histograms of radial positions.

Paths generated by FBM suffer from one significant shortcoming. In an enclosed volume, FBM will deplete the occupancy of particles near the boundary over time, resulting in a biased distribution. This phenomenon has also been reported by others (Vojta, Halladay, et al. 2020) and is not consistent with observations that chromosomal loci, unless associated with the nuclear envelope, localize at the nuclear periphery at a frequency expected from a random distribution (Brickner and Walter, 2004; Hediger et al., 2002). This may reflect a fundamental difference between sub-diffusion of particles and the apparent sub-diffusion of a segment of chromatin. We explored several methods to avoid depletion at the nuclear periphery. The following was effective: steps that would have taken the locus beyond the boundary were replaced with steps to the boundary along the same vector, and, upon interaction with the boundary, the normalized, correlated noise for future steps was regenerated (Fig. 3.1, Fig. 3.3). This modified simulation produced paths that closely matched the MSD, the distribution of positions within the nucleus, and the peripheral occupancy of nucleoplasmic chromosomal loci (Fig. 3.3 B, E–G; loci within 150 nm of the membrane in the simulation were scored as peripheral).

SIMULATING INTERACTION BETWEEN PARTICLE AND BOUNDARY

From our model for nucleoplasmic gene movement, we sought to simulate chromatin interaction with NPCs at the nuclear membrane. Based on the height of the NPC basket (Yang, Rout and Akey 1998, Vallotton, et al. 2019), we created a zone 50 nm from the boundary where chromatin could become 'bound,' causing it to switch to SPB-like sub-diffusion (Fig. 3.3 B). The probabilities of binding and unbinding within this zone were varied independently to optimize the agreement with the experimental MSD and peripheral localization (Fig 3.2, i.e., localization within 150 nm of the nuclear envelope) of *URA3:GRS1*. Based on this optimization, we found that a binding probability of 0.9 and a probability of remaining bound of 0.95 resulted in a positional distribution (Fig 3.2, Fig. 3.3 D), peripheral occupancy over time (Fig. 3.3 E, F), and MSD (Fig. 3.3 G) that most closely matched that of *URA3:GRS1*. We refer to this modified simulation as simulation+zip code. The fit of the simulation to the mean MSD for *URA3* and the simulation+zip code to the mean MSD for *URA3:GRS1* was excellent (Pearson's X^2 sums of 0.001 and 0.003, respectively, for t

from 0.21 to 4 s). Together, these two relatively simple simulations capture essential aspects of chromatin sub-diffusion and gene positioning at the nuclear periphery.

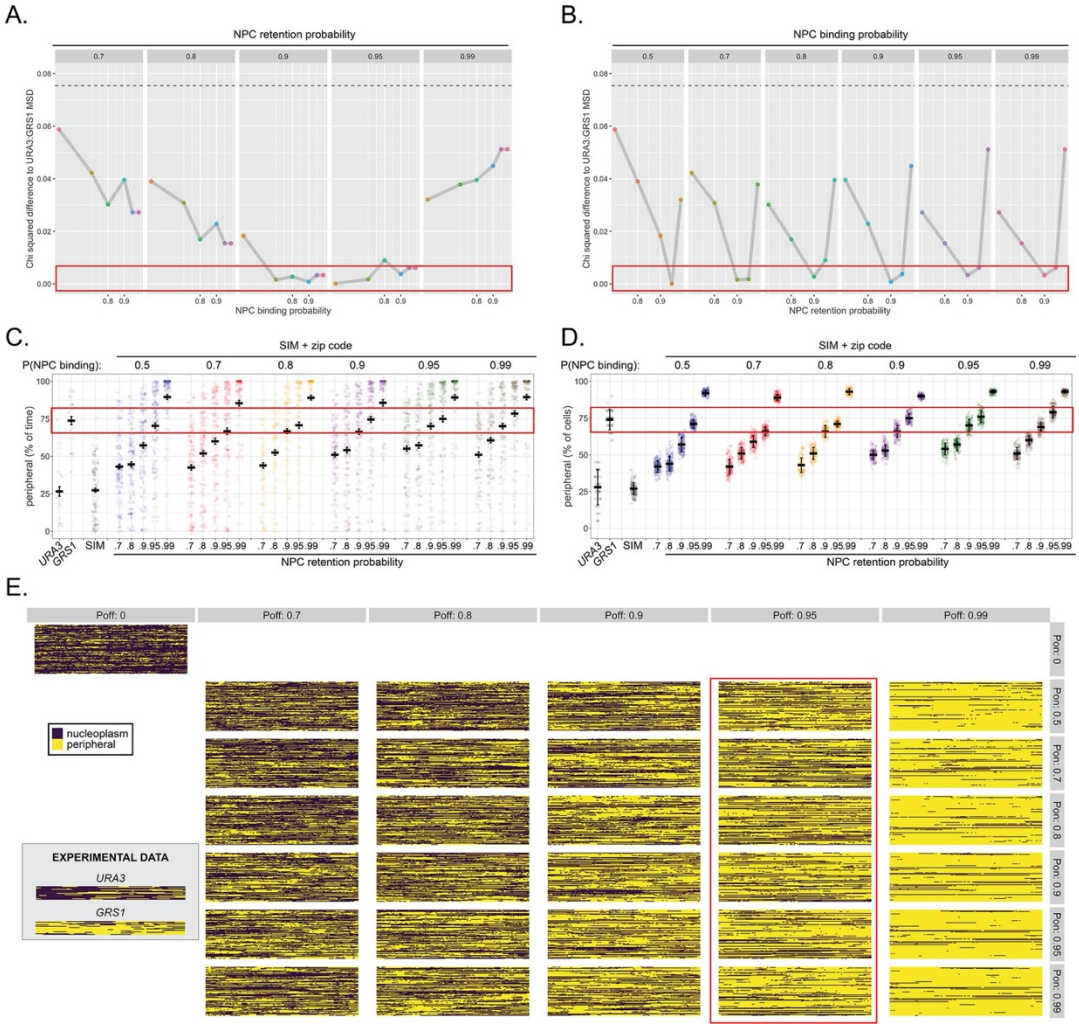

Figure 3.2 Determining association and dissociation parameters for two-state model to best simulate NPC-interacting chromosomal loci. The probability of binding and the probability of retention were independently varied and compared with the behavior of *URA3:GRS1*. (A, B) X^2 sum of differences between mean MSD plots of *URA3:GRS1* and each simulation ($\tau \leq 4$ s). Each panel represents a set of simulated paths with the indicated probability of remaining bound (A) or the probability of binding (B). Within each panel, the probability of binding (A) or remaining bound (B) was varied. The hatched line is the C-squared difference between the simulation with both binding and retention probabilities equal to zero and MSD of *URA3:GRS1*, for comparison. (C, D) Percent of time per cell (C) and the percent of cells at each time (D), that loci occupied the periphery (outer 150 nm shell of 1 μm radius nucleus) for *URA3*, *URA3:GRS1* (experimental observations from Fig. 2.3) and each combination of binding and retention probabilities. (E) Kymographs as in Fig. 2.3 (experimental data from Fig. 2.3 shown in inset), for each simulated combination of binding and retention probabilities. For all panels, red boxes highlight simulations similar to *URA3:GRS1* for the analyzed component.

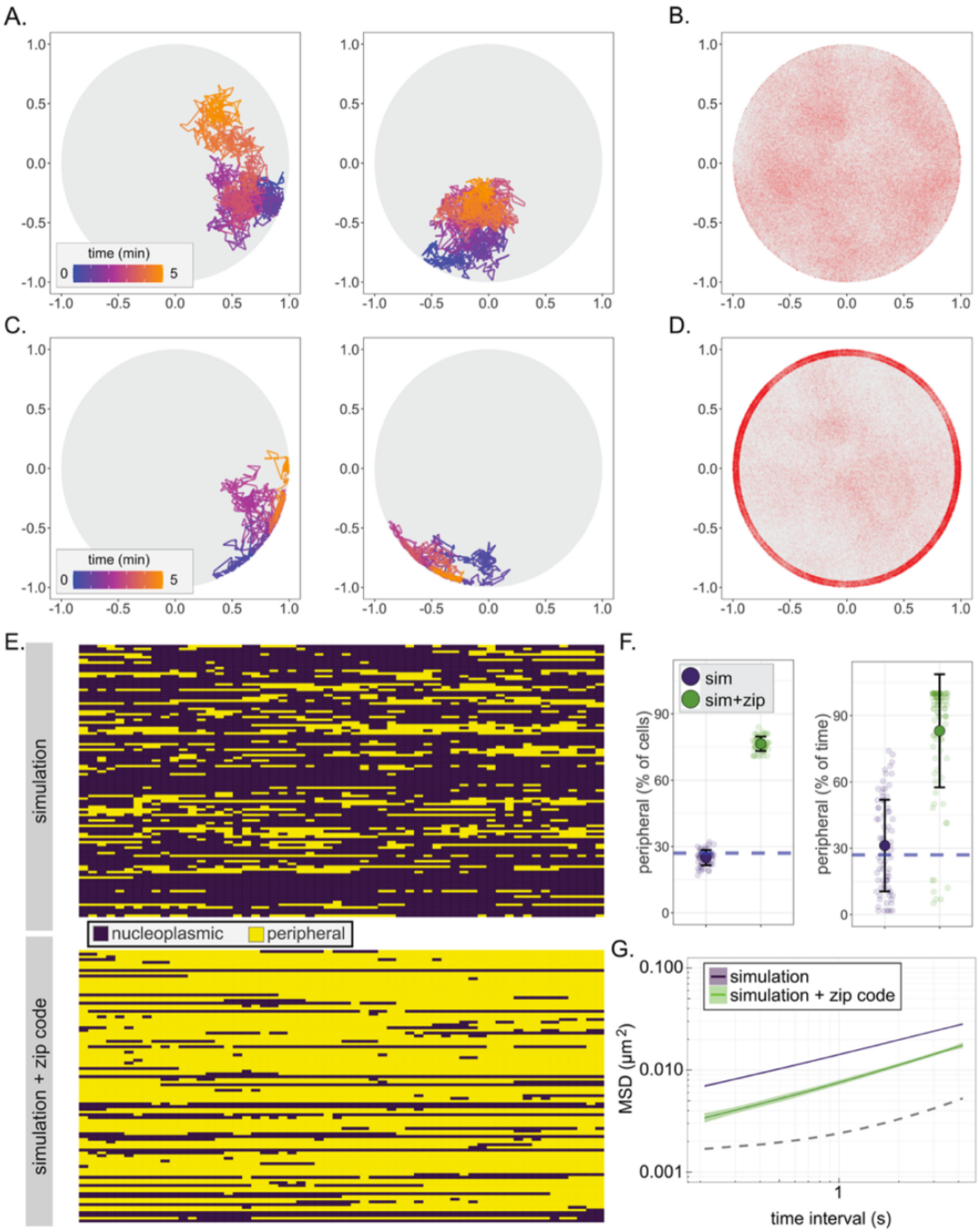

Figure 3.3 A fractional Brownian motion simulation of chromatin sub-diffusion. (A, C) Randomly selected example paths over 5 min at 200 ms time resolution. Color scale represents time. Paths were simulated using parameters (diffusion coefficient and anomalous exponent) extracted from a non-linear regression fit to *URA3* MSD (A; simulation) or by also allowing interaction at the nuclear envelope, slowing sub-diffusion to that of the SPB (C; simulation+zip code). (B, D) 150,000 positions visited in 100 simulated 5 min paths at 200 ms time resolution for the simulation (B) or the simulation+zip code (D). Peripheral localization (i.e., positioned <150 nm from the edge of the nucleus) every 10 s over 10 min for 100 paths from the simulation (top) and simulation+zip code (bottom). (F) Summary plots for percent of cells in that scored as peripheral at each time (left) or the percent of time each cell scored as peripheral (right) in either the simulation or the simulation+zip code. (G) MSD of the paths from the simulation or the simulation+zip code. Dark line is the mean, and the colored band represents the bootstrapped standard error.

With a functioning two state model that can reliably simulate chromatin trajectories we could start to generate hypotheses about the mechanism of movement used to translocate specific loci between the nucleoplasmic and peripheral regions. Seeing the frequency at which the simulation without a zip code was able to make first contact with the nuclear periphery, we proposed that translocation likely would not require directed, vectorial movement. As a comparison, generated simulations for super-diffusive particles took seconds for each trajectory to reach the periphery which was faster than any observed rate of peripheral localization. While we had no *in vivo* data that showed zip code dependent super-diffusive movement, it was important to have a hypothetical data set that could be compared to particle tracking from genes known to be undergoing translocation. Though these active trajectories were unlike any data we had quantified *in vivo*, it was still important to develop a new experimental method for us to generate trackable movies of gene translocation. But how could we ensure that movies were taken during translocation? To do this, we came up with techniques that could immediately bind positioning factors to a desired locus and monitor its position over time, as well as inhibiting proteins known to facilitate active movement in other sub-cellular systems (Myo3/Myo5). In the next section, it will be explained how we used these techniques to interrogate the necessity of these active movement components for localization and quantify movement during translocation.

CHROMATIN DYNAMICS DURING REPOSITIONING

Chromosomal loci can undergo long-range, directed movement (Mine-Hattab and Rothstein 2013), raising the possibility that repositioning from the nucleoplasm to the nuclear periphery could be an active process. Furthermore, actin and the myosin motor Myo3 have been shown to play a role in the localization of *INO1* to the nuclear periphery (Wang, et al. 2020). We find that deletion of Myo3 leads to a delay in the targeting of *URA3:INO1* to the nuclear periphery (Fig. 3.4 A, B). Importantly, this defect is specific to one (GRS I) of the two DNA zip codes that mediate repositioning of *INO1* to the nuclear periphery (Ahmed et al., 2010). When both zip codes (GRS I and GRS II) are present at the endogenous *INO1* gene, loss of Myo3 had no effect. Furthermore, once positioned at the nuclear periphery, *URA3:INO1* localization was unaffected by degradation of Myo3-AID (auxin-inducible degron; Fig. 3.4 C), suggesting that Myo3

increases the rate or efficiency of repositioning to the nuclear periphery. The MSD of *URA3:INO1* in the *myo3Δ* mutant reflected its localization; under repressing conditions or after only 1 hr of inositol starvation, the MSD was unchanged, whereas after 24 hr of inositol starvation, MSD decreased (Fig. 3.4 D). These results suggest that Myo3 impacts either the movement of *URA3:INO1* from the nucleoplasm to the nuclear periphery or other regulatory steps that are necessary for rapid GRS I-mediated peripheral localization.

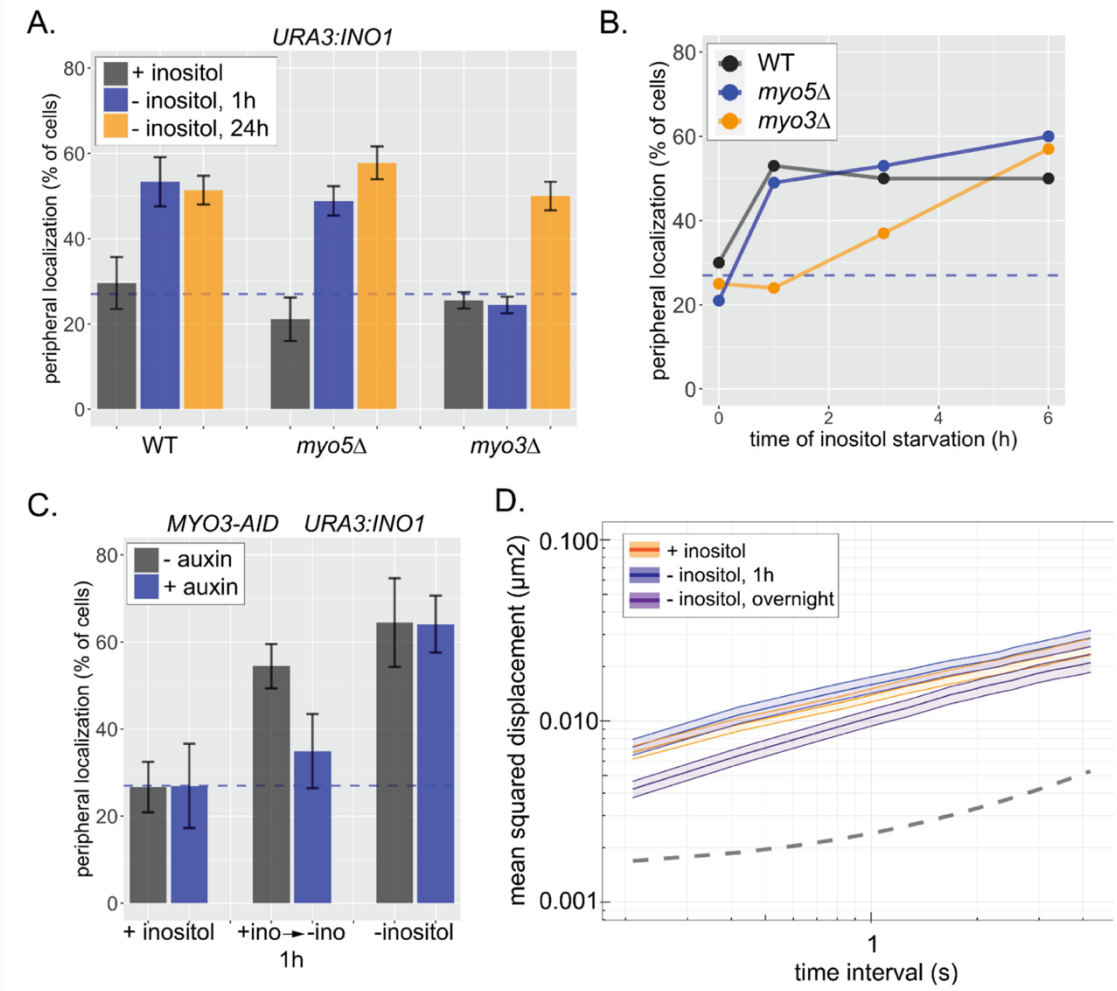

Figure 3.4 Loss of Myo3 delays GRS1-dependent repositioning to the nuclear periphery. The *URA3:INO1* locus (having GRS I but not GRS II) tagged with the LacO array shows GRS1-dependent localization to the nuclear periphery upon activation (Ahmed et al., 2010). (A) Wild- type, *myo5Δ*, and *myo3Δ* strains were scored for *URA3:INO1* gene positioning under repressing (+inositol) and activating conditions (either 1 hr or 24 hr -inositol). (B) Localization of *URA3:INO1* over time upon inositol starvation in wild-type, myo5Δ, and myo3Δ strains. (C) *URA3:INO1* localization in strains expressing Myo3 tagged with the auxin-inducible degron (AID) ±1 mM auxin for 1 hr under repressing conditions (+inositol) or under activating conditions (1 hr or 24 hr). In the case of the 1 hr -inositol condition, cells were pretreated with auxin for 1 hr before shifting into medium lacking inositol, with auxin. (D) MSD analysis of *URA3:INO1* in myo3Δ cells under repressing conditions (+inositol) or under activating conditions (1 hr or 24 hr).

To explore whether directed movement is responsible for the repositioning of genes from the nucleoplasm to the nuclear periphery, we first determined the simulation's behavior, which does not possess active, vectorial movement. Initiating either the default simulation of chromatin movement or the simulation+zip code from random positions within the nucleus, we followed the percent of the population showing localization within 150 nm of the nuclear edge over time. For the nucleoplasmic simulation, the peripheral localization remained random over time (~28% peripheral; Fig. 3.5 A). However, interaction with the nuclear envelope in the simulation+zip code resulted in stable repositioning to the nuclear periphery within ~2 min (Fig. 3.5 A). Therefore, rapid repositioning to the nuclear periphery can theoretically occur without any directed, active movement.

We applied live-cell tracking during repositioning from the nucleoplasm to the periphery to compare these simulations with experimental results. One challenge with such experiments is that the time required for genes to reposition when cells are shifted from uninducing to inducing conditions is gene-specific and can be relatively slow (e.g., t1/2 ~ 30min) (Brickner, Ahmed, et al. 2012, Brickner, Cajigas, et al. 2007, Randise-Hinchliff, et al. 2016). This suggests that the rate-limiting step for repositioning often reflects the regulation of transcription factors that mediate repositioning, rather than the rate-limiting step for movement to the periphery (Randise-Hinchliff, et al. 2016). To overcome this complication, we developed two approaches to maximize the rate of repositioning from the nucleoplasm to the nuclear periphery. First, we arrested cells bearing *URA3:GRS1*-LacO with α-factor mating pheromone, which disrupts peripheral localization by inhibiting Cdk, which phosphorylates Nup1 and is required for peripheral localization of *URA3:GRS1*. Upon release from a-factor arrest, *URA3:GRS1* repositioned to the nuclear periphery within ~15 min (Fig. 3.5 C).

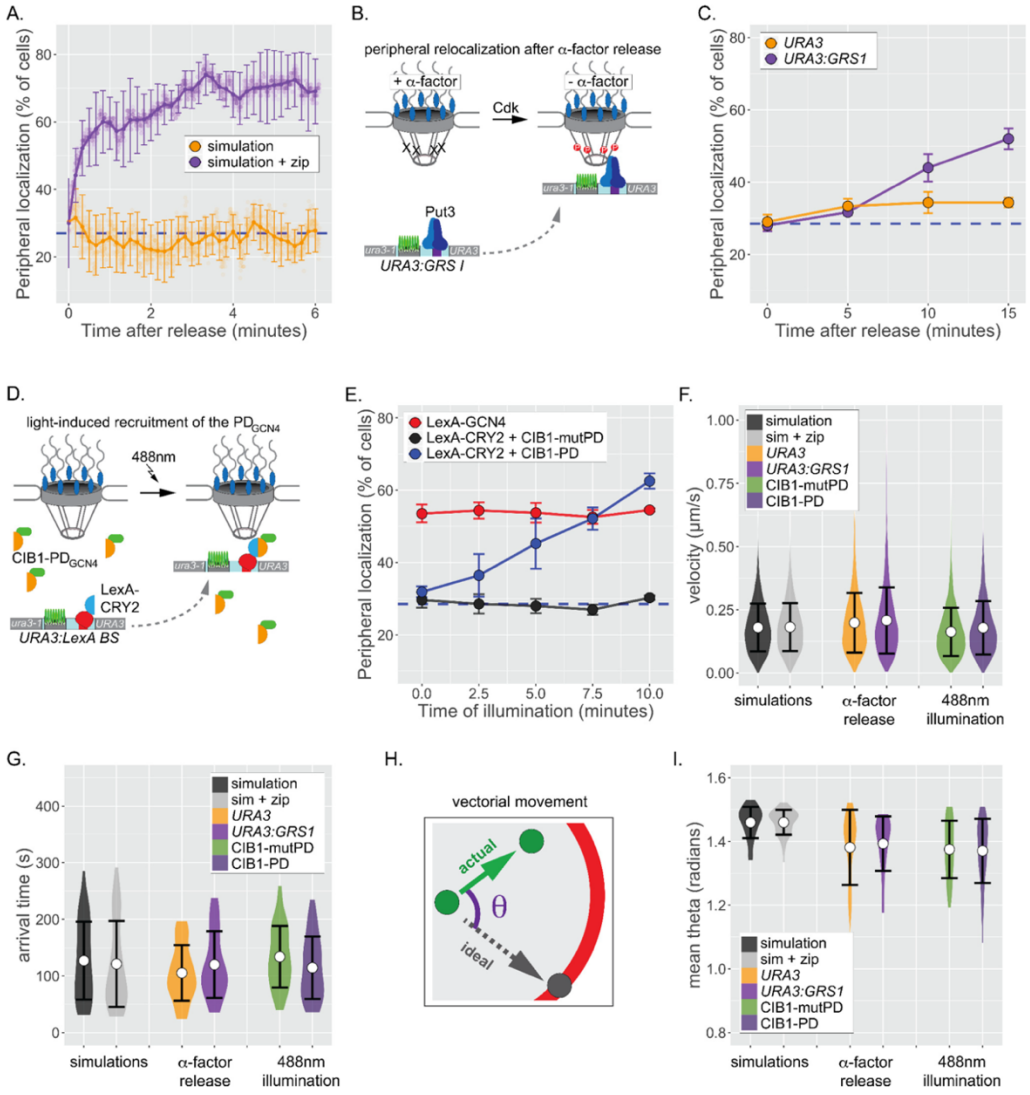

Figure 3.5 Repositioning from the nucleoplasm to the NPC. (A) Simulated repositioning. Simulated paths, using either the fractional Brownian simulation or the simulation+zip code, were initiated at random positions within 2 μm diameter nucleus and followed for 20 min (200 ms resolution). Colocalization with the periphery (i.e., < 150 nm from the edge) was scored for each simulation at each time and smoothed by averaging over 10 s windows. For each time point, three replicates of 33 paths were scored to generate an average (points) ± SEM (error bars). Blue, hatched line: peripheral localization expected for a random distribution. (B) Schematic for repositioning to the nuclear periphery upon release from a-factor arrest. (C) Peripheral localization (% of cells ± SEM) of *URA3* or *URA3:GRS1* over time after removing α-factor. (D) Schematic for optogenetic light-induced repositioning to the nuclear periphery. (E) Peripheral of *URA3:LexABS* in strains expressing either LexA-GCN4, LexA-CRY2+mutant PDGCN4-CIB1, or LexA-CRY2+wild- type PDGCN4 at the indicated times after illumination with 488 nm light. (F–I) Summary plots of velocity (F), arrival time (G), and angular deviation from an ideal path (I) from each cell before initial colocalization with nuclear periphery. White circles are the mean values, and error bars represent the standard deviation. For (F–I), simulated paths were initiated at random positions within a 1 μm diameter sphere in the center of the 2 μm diameter nucleus and followed for 5 min. Paths that did not make contact with the nuclear periphery were excluded.

Tethering of a 27 amino acid 'positioning domain' from the Gcn4 transcription factor (PDGCN4) near *URA3* using the LexA DNA binding domain (DBD) is sufficient to position U*RA3:LexABS* at the nuclear periphery (Brickner, Randise-Hinchliff, et al. 2019). Therefore, as a complementary approach, we used an optogenetic switch to recruit the PDGCN4 to *URA3*, resulting in targeting to the nuclear periphery. Cryptochrome 2 (CRY2) and cryptochrome interacting protein CIB1 from *Arabidopsis thaliana* undergo rapid dimerization when exposed to 488 nm light (Benedetti et al., 2018). In a strain having both the LacO array and the LexA binding site at *URA3*, CRY2-LexA DBD was co-expressed with CIB1-PDGCN4 to generate a light-induced peripheral localization system (Fig. 3.5 D) (Brickner et al., 2019). LexA DBD-Gcn4 served as a positive control and a mutant CIB1-pdGCN4 that does not mediate interaction with the NPC served as a negative control (Brickner et al., 2019). Cells were arrested, synchronized in G1, and illuminated with 488 nm light for 1 s pulses every 10 s over 10 min. Illumination resulted in rapid, PDGCN4-dependent repositioning to the nuclear periphery within ~7.5 min (Fig. 3.5 E). Thus, both the biological and the optogenetic stimuli led to rapid repositioning to the nuclear periphery with kinetics comparable to the simulation.

Having established that these two approaches lead to rapid peripheral localization, we then used particle tracking to define the nature of the movement during this transition. *URA3*, *URA3:GRS1*, or *URA3:LexABS* were tracked for 5 min at 0.5 s resolution (600 frames) during repositioning. For each movie, the position and time of initial colocalization with the nuclear envelope was recorded (if observed). While peripheral colocalization of *URA3:GRS1* and *URA3:LexABS*+CIB1-PDGCN4 represents – at least some of the time – interaction with the NPC, peripheral colocalization of the negative controls does not. Therefore, we expected that if directed movement brings genes to the nuclear periphery, the positive and negative controls should show differences in the step velocities, time of arrival, or directness of the path preceding arrival at the nuclear periphery. For comparison, we also determined each of these parameters for paths generated by the default simulation and the simulation+zip code, which include no directed movement. The mean velocities for the simulations and experimental controls were statistically indistinguishable, ranging from 0.163 ± 0.10 μm/s to 0.207 ± 0.13 μm/s (Fig. 3.5 F; n = 6077–9724 steps per strain), suggesting that the speed of movement was not increased during peripheral repositioning. We

did not observe significantly more large steps in the experimental movies than in the negative control movies (Fig. 3.5 F). The mean arrival time prior to initial contact with the nuclear envelope was also similar between the simulations and the experimental controls, ranging from 105 ± 49 s to 133 ± 54 s (Fig. 3.5 G; n = 27–40 cells per strain), consistent with the predictions from the simulation. Finally, to assess whether any of the loci underwent processive, vectorial movement during translocation, we measured the radial deviation of each step from a direct path to the ultimate contact point at the nuclear envelope (Fig. 3.5 H). Random sub-diffusion should produce an average θ of ~ 1.57 radians, while directed movement would produce an average of ~0. The simulations were close to random, and while the experimental loci appear slightly more directed than random, the positive and negative controls were indistinguishable (Fig. 3.5 I).

These results indicate that repositioning of chromatin from the nucleoplasm to the nuclear periphery is likely due to random sub-diffusion and collision with the NPC. This mechanism embodies an interesting paradox: a stochastic, indirect method of travel being used to organize and maintain positioning. In yeast, the rate of diffusion and size of the nucleus allows for a high likelihood of a gene colliding with the nuclear membrane at least once every few minutes despite maintaining a predominantly nucleoplasmic organization. In this way, the locus is simply primed for NPC capture through binding transcription factors without another mechanism directing the locus to a specific NPC. But this led to a final question, could our model help explain a more complex transcription-associated positioning phenomenon: inter-chromosomal clustering of similarly regulated genes following peripheral localization.

INTER-CHROMSOMAL CLUSTERING

Genes that interact with the yeast NPC can exhibit inter-allelic or inter-genic clustering with co-regulated genes (Brickner, Coukos and Brickner 2015, Brickner, Cajigas, et al. 2007, Brickner, Ahmed, et al. 2012, Brickner, Randise-Hinchliff, et al. 2019, Randise-Hinchliff, et al. 2016, Kim, Liachko, et al. 2017). Loss of specific nuclear pore proteins or transcription factors that bind to DNA zip codes disrupts clustering (Brickner, Ahmed, et al. 2012). Significant shortening of the distances between two inter-chromosomal loci within the population has been observed using fluorescent microscopy (Brickner, Ahmed, et al. 2012) and using biochemical methods such as 3C/HiC (Kim, Liachko, et al. 2017). To explore the dynamics of inter-

chromosomal clustering, we tracked the positions and inter-genic distances of well-characterized loci over time in live cells (Fig. 3.6 A). Both *HIS4* and *INO1* show inter-allelic clustering in diploids. Furthermore, inserting DNA zip codes at *URA3* induces clustering with *HIS4* (*URA3:GCN4BS*) (Randise-Hinchliff, et al. 2016) and *INO1* (*URA3:GRS1*) (Brickner, Ahmed, et al. 2012). The *URA3* gene, which does not undergo inter-chromosomal clustering (Brickner, Ahmed, et al. 2012), and pairs of randomly selected simulated paths served as negative controls.

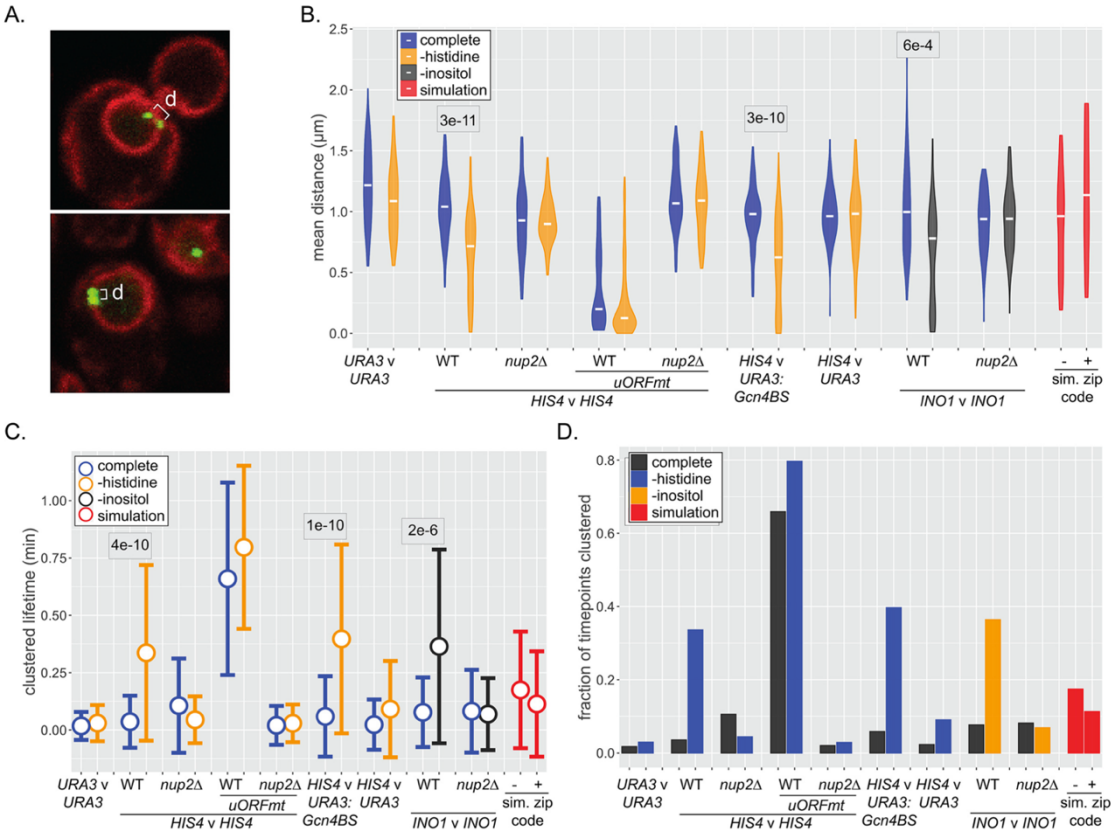

Figure 3.6 Dynamics of inter-chromosomal clustering. (A) Confocal micrographs of diploid cells with two loci marked with LacO arrays, expressing LacI- GFP and Pho88-mCherry. Distance between LacO arrays was measured over 200 x 200 ms time points in 40–50 cells (B–D). (B) Distribution of mean distances between loci for each cell, with the median for each strain or condition indicated with a white dash. p-values<0.05 from the Kolmogorov– Smirnov test are shown. (C) Distribution of lifetimes during which d < 0.55 μm. Dot = mean, error bars = SD. (D) The fraction of all time points that d < 0.55 μm for each strain and media condition. For (B–D), mean distances, the lifetimes, and fraction of timepoints clustered were also determined for pairs of randomly selected simulated paths (with or without zip code; red).

Similar to snapshots of populations, the distribution of mean distances from each cell over 40 s (200x0.21s) revealed clustering of *HIS4* with itself as well as inter-genic clustering of *HIS4* with *URA3:GCN4BS* upon histidine starvation (Fig. 3.6 B). Likewise, *INO1* inter-allelic clustering

was observed upon inositol starvation. Mutations in the upstream open reading frames that negatively regulate Gcn4 expression (*uORFmt*) (Mueller, Harashima and Hinnebusch 1987)), led to high-level, constitutive inter-allelic clustering of *HIS4* (Fig. 3.6 B) (Randise-Hinchliff, et al. 2016), while loss of Nup2 disrupted all clustering (Fig. 3.6 B). Finally, *URA3*, the simulated nucleoplasmic paths, and the simulated peripheral paths showed no clustering. Thus, NPC- and transcription factor-dependent clustering can be observed over time, and the simulated interaction with the NPC is not sufficient to produce clustering. This was an early indication that our simulation would also be unable to properly recreate the correlation of movement that could help maintain proximity between inter-chromosomal loci *in vivo*.

We also assessed the stability of clustering over time. The lifetimes of clustering (i.e., time two loci remain within 550 nm) increased from ~5 s for unclustered loci to 20–40 s upon clustering (Fig. 3.6 C). Similarly, the fraction of the total time points in which clustering was observed reflected the strength of clustering (Fig. 3.6 D). Because inter-chromosomal clustering persists for relatively long periods of time, it likely reflects a physical interaction, but the intermittent escape from the proximal distance indicates that this potential crosslinking is unstable and constantly being reestablished. But is this interaction responsible for just positional proximity between loci or able to coordinate movement between chromatin segments?

We analyzed whether pairs of loci that exhibit clustering show coordinated movement. To quantify the degree of coordination, we determined both the correlation of step sizes by each locus and the average difference in step angles made by each locus over 40 s movies (200 0.21 s; Fig. 3.7 A, B). Uncorrelated movement would result in a correlation of step sizes ~ 0 and a mean difference of angles of ~ $\pi/2 = 1.57$ radians for each movie, while perfectly coordinated movement would show a correlation of step sizes ~ 1 and a mean difference of angles ~ 0 (Fig. 3.7 C). Plotting the correlation and the mean difference in angle for many movies against each other gives a scatter plot (Fig. 3.7 C–L). As expected, randomly selected pairs of paths generated by the simulation or the simulation+zip code showed no correlated movement (Fig. 3.7 D). Likewise, nucleoplasmic *URA3* did not show correlated movement with itself or with *HIS4* (Fig. 3.7 J). However, strains that exhibit clustering (i.e., *HIS4* vs *HIS4*, *HIS4* vs *URA3:Gcn4BS*, or *INO1* vs *INO1*) showed a different pattern (Figure 3.7 E, G, and K). While the movement of loci that were >0.55 μm (orange dots) apart was uncorrelated, the subset of loci that were 0.55 μm (purple dots) showed correlated movement, both in terms of step size and angle. We quantified this behavior using the slope and R^2 of the

scatter plots (Fig. 3.7). Non-clustered control loci gave slopes ~ 0 and R^2 0.1 (e.g., Fig. 3.7 D, J). Under inducing conditions (but not under uninducing conditions), clustered loci gave a slope closer to the ideal slope of 1.57 and R^2 0.65 (Fig. 3.7 E, G, and K). Furthermore, overexpression of Gcn4 (*uORFmt*) increased coordinated movement (Fig. 3.7 H), while loss of Nup2 disrupted coordinated movement (Fig. 3.7 F, I, and L). Thus, interaction with the NPC, while not sufficient to cause clustering, is required for clustering and coordinated movement.

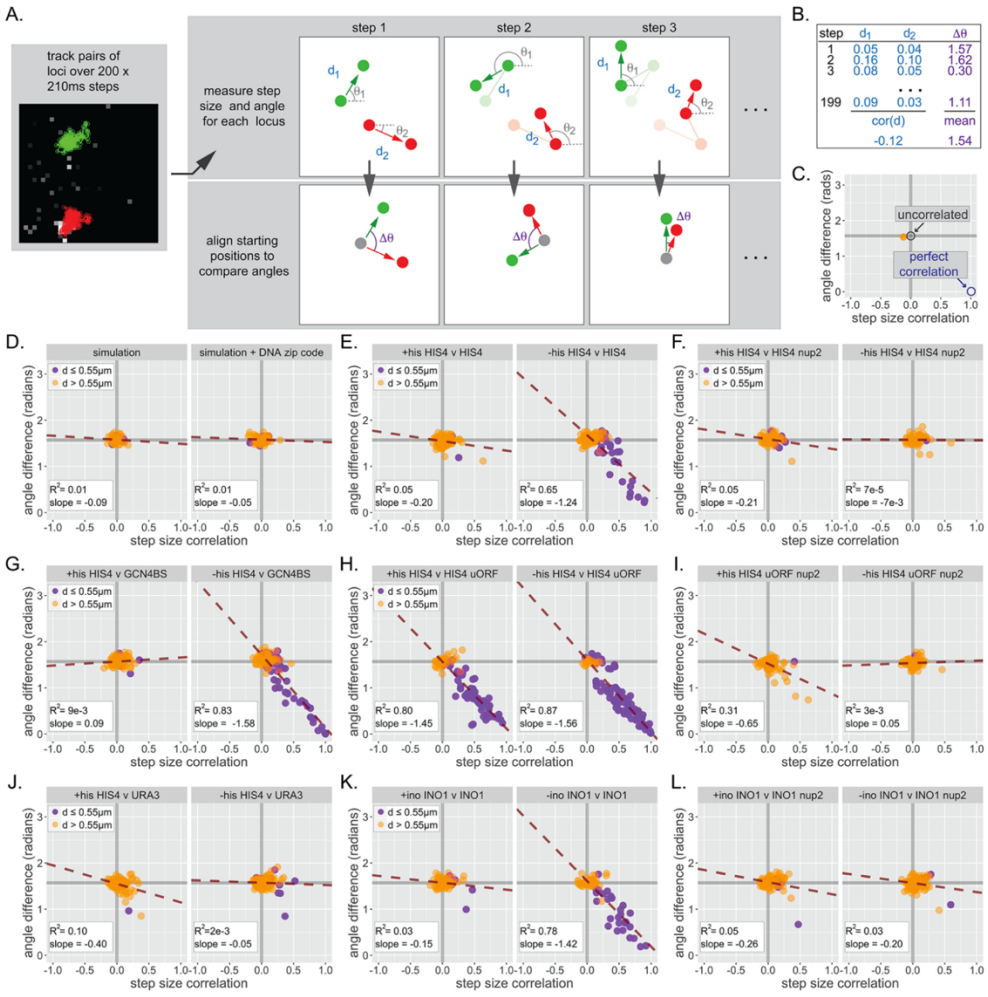

Figure3.7 Inter-chromosomal clustering leads to coordinated movement. (A) Workflow for tracking and analyzing movement of LacO array pairs. For each step from a time series, step distance and step angle are measured (top) and the difference in angles computed (bottom). (B) Each time series produces two values: a Pearson correlation coefficient (cor(d)) for all step sizes and a mean difference in angles ($\Delta\theta$). (C) Each cell produces a single point on the summary plot (orange). Gray lines highlight cor(d) = 0 and $\Delta\theta$ = p/2. Uncorrelated movement of two loci would be expected to cluster near cor(d) = 0 and $\Delta\theta$ = p/2, while perfectly correlated movement would result in cor(d) = 1 and $\Delta\theta$ = 0. (D–L) Summary plots for correlation analysis of the indicated pairs of loci in the indicated strains grown in the media described in the headers. Cells in which the mean distance between the loci was >0.55 μm appear in orange, while cells in which the mean distance between the loci was <0.55 μm appear in purple. For each plot, the slope and R^2 for a linear relationship between cor(d) and $\Delta\theta$ are indicated. Forty to 50 cells were analyzed per strain and condition. Simulations are the 50 pairs of paths generated for Figure 3.6

POTENTIAL MECHANSIMS AND ROLES FOR CLUSTERING

These results indicate that inter-chromosomal loci separated by hundreds of nanometers physically influence each other across hundreds of nanometers. But what can be inferred about the mechanism from our data? If there were a stable, physical cross-link between two loci, we would see almost all clustered loci having cor(d) ~ 1 and $\Delta\theta = 0$. But we instead observed very heterogenous cord(d) > 0 and $\frac{\pi}{2} > \Delta\theta > 0$ for genes that maintain proximity below 0.55 μm. This indicates either a local viscous environment with a selectively permeable barrier (i.e., phase separation) or a relatively high local concentration of transiently cross-linking proteins that interact with each other and chromosomal loci within a cluster. Our diffusion model is unable to recapitulate this clustering without added complexities that will likely require us to retool how our simulation handles interaction with the periphery.

Though inter-chromosomal clustering appears linked to transcriptional activation and peripheral localization, any biological purpose for this phenomenon remains hypothetical. Could this be a method to maintain a local concentration of RNA Polymerase II through unphosphorylated C-terminal domain phase separation (Boehning, et al. 2018) which would in turn increase transcription initiation? Conversely, clustering could sequester genes and control their expression through maintaining a ratio of RNA polymerase II relative to the number of genes present within the cluster. But to date, no data has conclusively shown that inter-chromosomal clustering influences yeast transcription. Within metazoan cells, inter-chromosomal clustering is an integral part of expression-related genome organization around nuclear structures, such as “nuclear speckle” transcription hubs, the nucleolus, and nuclear lamina (Quinodoz, et al. 2018). While a single metazoan hub could recruit hundreds of genes, the yeast clustering mechanism is limited to much fewer genes and could have a much more subtle effect on transcription regulation. To get at the mechanism and determine the purpose of clustering, improvements to data acquisition and analysis along with new tools for conditionally disrupting clustering will be invaluable for future work. Such details for future research on this phenomenon and the others contained in this dissertation are discussed within the final chapter.

CHAPTER 4

CONCLUSIONS AND FUTURE DIRECTIONS

Portions of this chapter were published in:

Sumner, M. C., Torrisi, S. B., Brickner, D. G., & Brickner, J. H. (2021). Random sub-diffusion and capture of genes by the nuclear pore reduces dynamics and coordinates inter-chromosomal movement. eLife, 10, e66238. doi:10.7554/eLife.66238

CONNECTING POSITION, NPC INTERACTION, AND TRANSCRIPTION

Tracking yeast NPC-associated chromatin over time revealed a frequent exchange between the nucleoplasm and periphery (Fig. 2.3), suggesting that the interaction with the NPC is continuously re-established and that population averages reflect this dynamism, rather than distinct, stable sub-populations. In other words, localization to the nuclear periphery involves a change in the steady-state positioning through continuous binding and dissociation. As interaction with the NPC enhances transcription (Ahmed, et al. 2010, Brickner, Randise-Hinchliff, et al. 2019, Brickner, Ahmed, et al. 2012, Brickner, Sood, et al. 2016, Capelson, et al. 2010, Liang, et al. 2013, Jacinto 2015, Taddei, et al. 2009) it is intriguing that the periodic and transient interaction with the NPC is reminiscent of the widespread phenomenon of transcriptional 'bursting' (Femino, et al. 1998, Rodriguez and Larson 2020). Perhaps the interaction with the yeast NPC functions with other transcriptional regulators to stimulate transcriptional bursts.

Future work should seek to correlate transcriptional bursts with gene positioning within the nucleus. For example, a system for visualizing nascent transcripts, such as the MS2 hairpin system (Tutucci 2018), could be utilized for simultaneous imaging of a LacO/LacI array and a nearby MS2-tagged gene. With proper controls, each image in a series will allow for both particle position and discrete quantifiable nascent transcript counting via relative fluorescence intensity. This combination of methods would provide an elegant and easily analyzable data set for determining whether frequency of contact with the nuclear periphery correlates with frequency of transcription initiation. Additionally, this method could be used to better determine how positioning affects robustness of reactivation following a poised memory state. At a

single cell level, a researcher would be able to compare MS2 intensities with the physical positioning of the locus of interest. Such experiments would likely require much longer time scales and necessitate a solution for keeping these cells from starving or inducing another stress response. Agar pads might be sufficient, but future work on developing an easy to produce microfluidic device would greatly improve acquisition efficiency and allow for much more interesting experiments. Capabilities for media switching, daughter harvesting, and monitored release from cell cycle synchronization would all greatly benefit a future experimentalist.

Prototyping such a system through conventional microfabrication would likely be costly and difficult to reliably produce devices on a timescale that would be conducive to rigorous and reproducible research (Crane, et al. 2014). As such, future molds for Polydimethylsiloxane (PDMS) cast microscopy culture devices can forgo the typical issues of small feature sizes and fragile photoresist layers deposited on a polished silicon wafer to instead use inverted vat Stereolithography (SLA) three-dimensional printing. Improvements to LCD screens and lifting mechanisms has pushed the resolution of SLA below 0.1 mm, making microfluidic channel molds quite easy to rapidly prototype. But this resolution is still much greater than the five-micron resolution attainable by conventional spin coat photoresist and photomask. As such, these channels would lack any small features that could act as yokes that would trap cells and allow them to be cultured on a slide. To circumvent this resolution issue, researchers have shown that priming devices with media containing concanavalin is sufficient to adhere yeast cells and capture single-cell fluorescence localization in a high-throughput manner (Hansen, Hao and O'Shea 2018). If no commercially available system for long term yeast culturing emerges within the next few years, developing such a device will likely become necessary for longer timescale movies and more intricate conditions occurring concurrently with acquisition.

A PASSIVE PROCESS FOR REPOSITIONING

Repositioning of genes to the NPC during transcriptional activation occurs over a wide range of timescales, depending on the stimulus and gene (Randise-Hinchliff, et al. 2016), making it difficult to test whether it involves super-diffusive or vectorial movement. Our simulated trajectories offer an essential

insight; starting from random positions within the center of the yeast nucleus, the population shifted from a random distribution to a peripheral distribution within ~2 min by random sub-diffusion. This timescale is comparable to the experimental models for peripheral repositioning (Fig. 3.5), arguing that active mechanism(s) are unnecessary to explain the observed rate of repositioning. More importantly, experimental analysis of the speed and vector of individual steps preceding contact with the nuclear envelope showed non-vectorial sub-diffusive movement that was indistinguishable from that captured by the simulation. Furthermore, there was no difference between experimental cells and negative control cells for these components. These results indicate that zip code-dependent gene localization results from random sub-diffusive chromatin movement, collision with the NPC, leading to dynamic binding. The recently discovered role for actin and Myo3 in localization of *INO1* at the nuclear periphery (Wang, et al. 2020) raises an important question: how do these factors impact peripheral repositioning through a sub-diffusive mechanism? Our results suggest that loss of Myo3 delays the arrival of some loci at the nuclear periphery but does not disrupt localization once it is established. Perhaps, like actin (Kapoor, et al. 2013), Myo3 impacts the function of chromatin remodeling complexes or histone-modifying enzymes, which regulate transcription factors binding to DNA zip codes (Randise-Hinchliff, et al. 2016). Alternatively, perhaps actin/Myo3 act at the NPC to facilitate capture. A better biochemical and biophysical understanding of these processes will illuminate such possible roles.

Interaction with nuclear pore proteins plays a conserved role in promoting transcription. However, while the interaction of yeast genes with nuclear pore proteins occurs at the nuclear periphery in association with the NPC, many genes in mammalian cells and *Drosophila* interact with soluble nuclear pore proteins in the nucleoplasm (Capelson, et al. 2010, Liang, et al. 2013, Light, Freaney, et al. 2013). Sub-diffusion for mammalian chromatin (which has been suggested to be less mobile than in yeast) (Chubb, et al. 2002) in a nucleus with a radius of 5 μm would make it impossible (on a biologically meaningful timescale) for loci in the center of the nucleus to reach the periphery. In larger nuclei, recruitment of nuclear pore proteins to sites of action, regardless of their position, likely overcomes this obstacle.

Both the α-factor release and light-induced dimerization system are valuable tools for future interrogation of the repositioning mechanism. While we used an endogenous and artificial approach, we only assayed the effects of Put3 and GCN4PD mediated repositioning. To get a more complete picture of

potential changes in dynamics during repositioning, these tools should be expanded to other positioning factors and domains. While the data presented here shows a purely stochastic, passive mechanism, there could very well be heterogenous mechanisms for localization or unique cases that do utilize an active mechanism. Because peripheral localization appears to be a very common effect of transcription factor binding, there remains a high possibility of multiple mechanisms facilitating translocation at different loci until the movement of a locus tethered to each known positioning factor is screened for diffusion dynamics. The currently employed LexA dimerizer system is well suited for testing this exact type of screen that could be acquired in an automated manner for excitation and acquisition cycles.

INTERROGATING THE CLUSTERING MECHANISM

Inter-chromosomal clustering is a widespread phenomenon in eukaryotes (Bantignies, et al. 2011, Brickner, Ahmed, et al. 2012, Cook and Marenduzzo 2018, Gehlen, et al. 2012, Haeusler, et al. 2008, Noma, et al. 2006, Ramos, et al. 2006, Taddei, et al. 2009, Thompson, et al. 2003, Xu and Cook 2008). Genes that interact with the NPC through shared transcription factors exhibit inter-chromosomal clustering (Brickner, Ahmed, et al. 2012, Brickner, Sood, et al. 2016, Kim, Liachko, et al. 2017, Randise-Hinchliff, et al. 2016). Such clustering requires transcription factor(s) and nuclear pore proteins (Brickner, Ahmed, et al. 2012, Kim, Liachko, et al. 2017, Chowdhary, Kainth and Gross 2017) but is also mechanistically distinguishable from interaction with the NPC (Brickner, Sood, et al. 2016). Clustering persisted for 20–40 s and led to correlated movement between pairs of loci that were within 550 nm. Importantly, independently correlating step size and step angle is sensitive to correlations among pairs of loci in a subset of the cells in the population. Such correlated movement, averaged over the entire population, would be more challenging to appreciate. This may explain why previous work tracking movement of pairs of active GAL1-10 alleles in yeast found little correlation in aggregate (Backlund, et al. 2014). Pairs of paths generated by either the simulation or the simulation+zip code do not lead to inter-chromosomal clustering, consistent with the observation that genes that interact with the NPC through different transcription factors do not exhibit clustering (Brickner, Ahmed, et al. 2012). Therefore, while clustering requires transcription factors and interaction with the NPC, it represents a distinct physical interaction. Surprisingly, the correlated movement

was observed between loci separated by hundreds of nanometers, suggesting that it reflects a large molecular complex, or more likely, an environment. Physical interactions that lead to phase separation could encompass groups of genes to create a (perhaps transient) nuclear sub-compartment (Hult, et al. 2017). This is reminiscent of super-enhancers which exist within phase-separated droplets (Hnisz, et al. 2017, Sabari, et al. 2018) and are strongly associated with nuclear pore proteins (Ibarra, et al. 2016). Phase separation may be facilitated by multivalent interactions between natively unstructured nuclear pore proteins, which are capable of forming phase-separated droplets *in vitro* (Frey and Gorlich 2007). Such conditional phase separation would be regulated and specified by transcription factors, and potentially other transcriptional complexes such as mediator or RNA polymerase II, to functionally compartmentalize the nucleus. Unpublished data has also implicated Nup2 in the maintenance of inter-chromosomal clusters, not just the initial formation. Techniques that disrupt peripheral localization but maintain inter-chromosomal clusters have identified that Nup2 may have a role in cluster maintenance away from the NPC. This is quite an exciting finding as it represents the first potential soluble Nup role in *S. cerevisiae*, through it requires a potentially artificial scenario (drug treatment and conditional knockouts) to become observable

Single particle tracking is a relatively simple process that can be achieved through many different methods depending on an operator or analyst's level of coding and software capabilities. But clustering analysis requires tracking multiple particles across a multi-dimensional acquisition which can present a problem that is orders of magnitude more difficult to solve than a single particle. A dedicated researcher could likely develop a more widely applicable tracking software to handle multiple cells and multiple loci within a single cell without an operator performing manual segmentation. This should allow for more high-throughput screening of clustering phenotypes and more reliable tracking of multiple loci from different cells in the same acquisition. Both of which would save considerable time compared to the current methodology of single-cell movies and partially automated analysis. Established methods such as radial particle tracking (Kashkanova, et al. 2021) or real-time tracking (Hou, Exell and Welsher 2020) can be synthesized to better differentiate clustered loci and potentially allow for deconvolution of greater than two loci being tracked simultaneously to better understand the actual number of genes occupying inter-chromosomal clusters.

MODELING DIFFUSION

Chromatin undergoes anomalous sub-diffusive movement during interphase (Hajjoul, et al. 2013, Marshall, et al. 1997). The physical interaction between chromatin and the NPC, though transient, reduces chromatin sub-diffusion (Fig. 2.4) (Backlund, et al. 2014, Cabal, et al. 2006) independent of changes in transcription (Fig. 2.6). Using the parameters derived from MSD, we developed computational simulations for yeast chromatin sub-diffusion in the nucleoplasm and at the nuclear periphery. The anticorrelation between successive steps of chromatin can be modeled as FBM (a.k.a. overdamped fractional Langevin motion) (Lucas, et al. 2014). Sub-diffusion of yeast chromosomal loci is determined by the elastic response from the chromatin polymer and the viscous interaction between the polymer and the nucleoplasm. While we do not explicitly simulate the total chromatin polymer or other nuclear occupants, FBM captures their net effects, recapitulating the MSD behavior of a nucleoplasmic locus. However, the FBM model leads to exclusion near boundaries, leading to non-random positioning of loci, a phenomenon that is not consistent with experimental observations. This likely reflects the fact that, while the motion of a segment of chromatin can be modeled as an FBM particle, it is part of a polymer and is not an FBM particle. Our solution to this shortcoming of the FBM model, recalculating the path upon collision with the nuclear boundary (see detailed explanation in Materials and methods), produced localization patterns and MSD behaviors that are consistent with experimental observations.

To simulate the interaction of chromatin with the NPC, we allowed loci in an area within 50 nm of the nuclear boundary to ‘bind’ to the nuclear periphery, assuming the mobility of the SPB. The width of this annulus is roughly equal to the height of the NPC nuclear basket (Vallotton, et al. 2019) whose components are required for chromatin association with the NPC (Ahmed, et al. 2010). We independently optimized the probability of binding and of remaining bound by comparing the positioning and MSD of simulated paths with that conferred by a DNA zip code. This simple modification of the simulation was able to reliably recreate the peripheral localization and constraint on chromatin sub-diffusion caused by interaction with the NPC (Fig. 3.3). Thus, the work described here provides a straightforward and robust theoretical framework

for modeling the biophysical nature of gene positioning through association with any stable nuclear structure.

While the regeneration complexity was able to solve boundary avoidance in our simulated trajectories, it is still a conservative assumption that was successful in recapitulating our *in vivo* data. But such an assumption is neither based on nor explains the underlying mechanism. To better simulate this phenomenon, two things must be achieved: finer sampling of chromatin movement at the periphery and a new approach to the underlying step process within the simulator. For finer data acquisition, a more complete analysis of chromatin movement relative to distance from the periphery, similar to Fig. 2.5, could uncover a unique mode of movement that only occurs within proximity to the nuclear boundary that is somehow different from our homogenous nucleoplasmic diffusion. Analyzing this data could very well uncover how the sub-diffusive movement of chromatin maintains boundary proximity. Additionally, while FBM provided a robust method for trajectory simulation, a process which takes the imposed boundary into account before simulation could replace the need for repetitive trajectory regeneration. Recent approaches that utilize solving the fractional Langevin equation can generate FBM trajectories with boundaries in mind that have varying degrees of force absorption (Vojta and Warhover 2021, Salem and Alnegga 2020). This would allow for more discrete control of boundary collision and will likely require our source code for the stepper to be rewritten in a precompiled language or utilizing the *numba* package within Python to ensure fast simulations that would not be too computationally intensive for a future researcher's computer

Increasing the throughput of data for both transcriptional bursting and clustering analysis will provide even more opportunities to further tune our gene diffusion model and better simulate not just a single particle, but how multiple particles within a cluster influence each other's movement. The current fractional Brownian motion model works very well for simulating a single gene locus but becomes vastly more computationally intensive when scaled up to even just two particles. A new approach for modeling multiple particles is already being developed that instead uses a pre-compiled language to act as a fractional Langevin equation solver that could better account for the overall trajectories multiple particles would undergo and provide a new opportunity to adjust how nuclear boundary collisions are handled. But this change in modeling would be best served with either higher resolution data than currently available or a new immense data set of individual gene positions and genes undergoing clustering to test and train

against. This work sets up a future researcher to unify the changes in sub-diffusive movement with a potential mechanism for inter-chromosomal clustering. But whether they can improve acquisition sensitivity and analysis processivity will largely determine the success of that research and the project's completion on a reasonable timescale.

MATERIALS AND METHODS

Chemicals, reagents, and media

All chemicals were purchased from Sigma-Aldrich unless otherwise noted. Media components were from Sunrise Science Products, and a-factor was from Zymo Research. Yeast and bacteria media and transformations were as described (Burke, Dawson and Stearns 2000, Wood, et al. 1983).

Yeast strains

All yeast strains were derived from W303 (ade2-1 ura3-1 trp1-1 his3-11,15 leu2-3,112 can1-100) strains CRY1 (MATa) or CRY2 (MATa; Brickner and Fuller, 1997) and are listed in Supplementary file 2. The μNS cytoplasmic particle was expressed from plasmid pAG415GPD EGFP-μNS (Munder et al., 2016).

Yeast culturing

Yeast cultures were inoculated from a YPD agar plate into synthetic dextrose complete (SDC) or drop out media (Burke et al., 2000) and rotated at 30 ˚C for 18 hr, diluting periodically to maintain the cultures at OD600 <0.8. Before MSD tracking microscopy, cultures were diluted to 0.1 OD/mL and treated with 2 ng/mL of nocodazole for 2 hr. Cultures were then pelleted, washed, and resus pended in SDC to release from M-phase into G1-phase for 10 min. Cells were then pelleted again, concentrated, applied to a microscope slide, and covered with a glass coverslip for imaging.

For experiments involving mating pheromone, 100 mM a-factor was added to the cultures following release from nocodazole arrest for 30 min. To release from pheromone arrest, cells were pelleted, washed into SDC, and mounted for microscopy.

Microscopy

Confocal microscopy was performed in the Northwestern University Biological Imaging Facility. Tracking microscopy was performed on a Leica Spinning Disk Confocal Microscope (Leica DMI6000

inverted microscope equipped with Yokogawa CSU-X1 spinning disk and Photometrics Evolve Delta512 camera), and static localization experiments were performed on a Leica TCS SP8 Confocal Microscope.

For both single locus/particle MSD and multiple loci tracking, the same acquisition protocol was used. GFP-LacI/LacO spots in G1-phase cells were imaged every 210 ms for 200 frames in a single z plane with a minimum of 40 biological replicates per experimental condition. Cells that did not remain immobilized or whose loci underwent no movement were excluded from our analysis. For peripheral relocalization dynamics experiments, LacI-GFP/LacO128 arrays in G1-phase cells were imaged every 500 ms for 600 frames and Pho88-mCherry was imaged every 10 s to determine the position with respect to the nuclear periphery (D'Urso et al., 2016; Egecioglu et al., 2014).

Static localization experiments were acquired as z-stacks encompassing the full yeast cell, and 30–50 cells were scored per biological replicate as described (Brickner et al., 2010; Brickner and Walter, 2004; Egecioglu et al., 2014). Each strain and condition included at least three biological replicates. To activate light induced recruitment, cells were scanned with the 488 nm laser every 10 s.

Particle tracking and data analysis

Tracking was performed using the ImageJ plugin MTrackJ. To accommodate clustering experiments (which typically have two or more fluorescent particles per nucleus), MTrackJ's region of tracking tool was utilized to ensure the signals from individual loci were tracked separately. Tracking data was output as a comma-separated text file and analyzed with R scripts available via GitHub. (https://github.com/MCnu/R_sim_scripts). Repositioning analysis utilized a lookup table that contained the frame and the position in which the signal from LacI-GFP/LacO128 array of a given cell first colocalized with the Pho88-mCherry nuclear membrane signal.

Statistical methods are defined within each figure legend where employed. All code used to perform statistical analysis is included within referenced source code and utilized the R packages *stats, data.table,* and the *tidyverse* meta-package collection. MSD paramaters were extracted from MSD curves using the non-linear regression function nls() using the simplified MSD formula (Eq. 3.1).

FBM simulations

We model the dynamics of chromosomal loci in the cellular nucleus via a discrete-time random walk with continuously varying step sizes. This simulation is governed by FBM, which gives rise to

anomalous diffusion of the locus. Anomalous diffusion is distinct from Brownian diffusion due to a non-linear MSD over time, with distinct behaviors for the super-diffusive (α > 1) vs. sub-diffusive (α < 1) regimes. Free fitting our MSD measurements for 23 different loci/conditions, we found an average α = 0.52 (not shown), matching that determined in previous work (Hajjoul et al., 2013). Therefore, for the simulations, we used α = 0.52. Following previous work (Lucas et al., 2014), we present fractional Langevin dynamics simplified by the assumption of overdamping (i.e., no inertial term) and no driving force. In FBM, the statistical noise is a stationary Gaussian process with a mean equal to zero and a nonzero anticorrelation between successive steps (Meyer, Sellan and Taqqu 1999). This property is exploited to allow random vector generation with a given correlation structure (Dietrich and Newsam 1997). We draw values for each simulated dimension of movement to generate the entire time series for a trajectory. We re-scale the vectors to an appropriate magnitude for given time units equal to t using a Γ parameter provided by non-linear regression on experimental MSD data (where MSD (t) = $\Gamma(t^{0.52})$). No additional complications in our computational model are required to reproduce experimental MSD/

To properly simulate chromatin diffusion within the confines of the nucleus, we added an impassable boundary to serve as a nuclear membrane. Recent work on the behavior of FBM and the fractional Langevin equation in finite volumes of space showed that the presence of boundaries and the handling of those boundary conditions can affect the long-timescale distribution close to the edges of the domain (Guggenberger, et al. 2019, Vojta, Halladay, et al. 2020)These studies agree with our findings that in the sub-diffusive regime, depletion occurs at the boundary. This depletion at the periphery is rationalized by the fact that because successive steps are anticorrelated, a step that would take the particle over the boundary is likely to be followed by one which would take it away from it. Such depletion is not observed in experimental distributions of control and non-control specimens. It is possible that the physicochemical landscape of the periphery or the region near the periphery involves many interactions which have the effect of attracting the chromatin locus to the periphery, but such effects are not evident in the aforementioned studies (which do not consider transient binding interactions with a hard wall). Because our particle is a segment of a much larger polymer in reality, we instead decided to regenerate the underlying noise time series whenever the trajectory collides with the periphery to negate the effects of prior

movement. This adaptation succeeded in creating a uniform distribution of positions across the nucleus. However, we acknowledge that our theoretical particle no longer satisfies the fluctuation dissipation theorem inherent to all Brownian motion, including FBM. Additional investigation of the behavior of chromatin at the boundary in silica and in vivo will help clarify the validity of this modification.

Binding of chromatin to NPCs was modeled using a simple two-state Markov model wherein a locus within the peripheral region (an annulus extending 50 nm from the nuclear boundary) can assume a bound state in the next step with a defined probability. Particles bound to the NPC remain bound at a second defined probability for every step until it becomes unbound. A particle bound to the NPC is assumed to be interacting strongly with an NPC, their motion is inhibited, but not entirely arrested. We therefore scaled the step sizes of particles in the bound state with Γ and α parameters derived from non-linear regression of the MSD for the SPB. In this way, we simulate the effective 'pausing' of chromatin motion due to NPC interaction.

Source code

Our simulation data and source code are openly available. Our simulations were implemented in Python, with routine algorithms like random noise generation or the fast Fourier transform from the NumPy library (Harris et al., 2020), and all other codes implemented using custom libraries are available on GitHub (https://github.com/MCnu/YGRW). Analytical pipeline of two-dimensional tracking data is also available. All analyses were implemented in R, and scripts are available on GitHub (https://github.com/MCnu/R_sim_scripts).

REFERENCES

Ahmed, S, DG Brickner, WH Light, I Cajigas, M McDonough, AB Froyshteter, T Volpe, and JH Brickner. 2010. "DNA zip codes control an ancient mechanism for gene targeting to the nuclear periphery." *Nat Cell Biol* doi:10.1038/ncb2011.

Arbona, JM, S Herbert, E Fabre, and C Zimmer. 2017. "Inferring the physical properties of yeast chromatin through bayesian analysis of whole nucleus simulations." *Genome Biology* doi:10.1186/s13059- 017-1199-x .

Arndt, K, and GR Fink. 1986. "GCN4 protein, a positive transcription factor in yeast, binds general control promoters at all 5′ TGACTC 3′ sequences." *Proc. Natl. Acad. Sci.* doi:10.1073/pnas.83.22.8516.

Avşaroğlu, B, G Bronk, S Gordon-Messer, J Ham, DA Bressan, JE Haber, and J Kondev. 2014. "Effect of chromosome tethering on nuclear organization in yeast ." *PLoS ONE* doi:10.1371/journal.pone.0102474 .

Backlund, MP, R Joyner, K Weis, and WE Moerner. 2014. "Correlations of three-dimensional motion of chromosomal loci in yeast revealed by the double-helix point spread function microscope." *Molecular Biology of the Cell* doi:10.1091/mbc.e14-06-1127.

Bantignies, F, V Roure, I Comet, B Leblanc, B Schuettengruber, J Bonnet, V Tixier, A Mas, and G Cavalli. 2011. "Polycomb-dependent regulatory contacts between distant hox loci in Drosophila." *Cell* doi:10.1016/j.cell.2010.12.026.

Batsios, P, T Peter, O Baumann, R Stick, I Meyer, and R Gräf. 2012. "A lamin in lower eukaryotes?" *Nucleus* doi: 10.4161/nucl.20149.

Blobel, G. 1985. "Gene gating: a hypothesis." *Proc Natl Acad Sci* doi: 10.1073/pnas.82.24.8527.

Boehning, M, C Dugast-Darzacq, M Rankovic, A Hansen, X Darzacq, and M Zwekstetter. 2018. "RNA polymerase II clustering through carboxy-terminal domain phase separation." *Nat Struct Mol Biol* doi:10.1038/s41594-018-0112-y.

Boumendil, C, P Hari, KC Olsen, JC Acosta, and WA Bickmore. 2019. "Nuclear pore density controls heterochromatin reorganization during senescence." *Genes & Dev* doi: 10.1101/gad.321117.118.

Brickner, DG, and JH Brickner. 2010. "Cdk phosphorylation of a nucleoporin controls localization of active genes through the cell cycle." *MBoC* doi: 10.1091/mbc.E10-01-0065.

Brickner, DG, C Randise-Hinchliff, ML Corbin, JM Liang, S Kim, B Sump, A D'Urso, et al. 2019. "The role of transcription factors and nu- clear pore proteins in controlling the spatial organization of the yeast genome." *Dev Cell* doi:10 .1016/j.devcel.2019.05.023.

Brickner, DG, I Cajigas, Y Fondufe-Mittendorf, S Ahmed, PC Lee, J Widom, and JH Brickner. 2007. "H2a.Z-mediated localization of genes at the nuclear periphery confers epi-genetic memory of previous transcriptional state." *Plos Biol* doi:10.1371/journal.pbio.0050081.

Brickner, DG, R Coukos, and JH Brickner. 2015. "INO1 transcriptional memory leads to DNA zip code-dependent interchromosomal clustering." *Microbial Cell.*

Brickner, DG, S Ahmed, L Meldi, A Thompson, WH Light, M Young, TL Hickman, F Chu, E Fabre, and JH Brickner. 2012. "Transcription factor binding to a DNA zip code controls interchromosomal clustering at the nuclear periphery." *Dev Cell* doi:10.1016/j.devcel .2012.03.012.

Brickner, DG, V Sood, E Tutucci, R Coukos, K Viets, RH Singer, and JH Brickner. 2016. "Subnuclear positioning and interchromosomal clustering of the GAL1-10 locus are controlled by separable, interdependent mechanisms." *Mol Biol Cell* doi:10.1091/mbc.E16-03- 0174.

Brickner, JH, and P Walter. 2004. "Gene recruitment of the activated INO1 locus to the nuclear membrane." *Plos Biol* doi:10.1371/journal.pbio.0020342.

Brown, JM, J Green, RP das Neves, HA Wallace, AJ Smith, J Hughes, N Gray, S Taylor, WG Wood, and DR Higgs et al. 2008. "Association between active genes occurs at nuclear speckles and is modulated by chromatin environment." *J Cell Biol* doi:10.1083/jcb.200803174.

Burke, D, D Dawson, and T Stearns. 2000. "Methods in Yeast Genetics." *Cold Spring Harbor Laboratory.*

Cabal, GG, A Genovesio, S Rodriguez-Navarro, C Zimmer, O Gadal, A Lesne, H Buc, F Feuerbach-Fournier, JC Olivo-Marin, and EC Hurt. 2006. "SAGA interacting factors confine sub-diffusion of transcribed genes to the nuclear envelope." *Nature* doi:10.1038/nature04752.

Callan, HG, and SG Tomlin. 1950. "Experimental studies on amphibian oocyte nuclei. I. Investigation of the structure of the nuclear membrane by means of the electron microscope." *Proceedings of the Royal Society of London. Series B, Biological sciences* 10.1098/rspb.1950.0047.

Capelson, M, Y Liang, R Schulte, W Mair, U Wagner, and MW Hetzer. 2010. "Chromatin-bound nuclear pore components regulate gene expression in higher eukaryotes." *Cell* doi:10.1016/j.cell.2009.12.054.

Casolari, JM, CR Brown, DA Drubin, OJ Rando, and PA Silver. 2005. "Developmentally induced changes in transcriptional program alter spatial organization across chromosomes." *Genes Dev* doi:10.1101/gad.1307205.

Casolari, JM, CR Brown, S Komili, J West, H Hieronymus, and PA Silver. 2004. "Genome-wide localization of the nuclear transport machinery couples transcriptional status and nuclear organization." *Cell* doi:10.1016/ S0092-8674(04)00448-9.

Chowdhary, S, AS Kainth, and DS Gross. 2017. "Heat shock protein genes undergo dynamic alteration in their Three Dimensional structure and genome organization in response to thermal stress." *Molecular and Cellular Biology* doi:10.1128/MCB.00292-17.

Chubb, JR, S Boyle, P Perry, and WA Bickmore. 2002. "Chromatin motion is constrained by association with nuclear compartments in human cells ." *Current Biology* doi:10.1016/S0960-9822(02) 00695-4 .

Cook, PR, and D Marenduzzo. 2018. "Transcription-driven genome organization: a model for chromosome structure and the regulation of gene expression tested through simulations." *Nucleic Acids Research* doi:10.1093/nar/gky763.

Crane, MM, IBN Clark, E Bakker, S Smith, and PS Swain. 2014. "A Microfluidic System for Studying Ageing and Dynamic Single-Cell Responses in Budding Yeast ." *PLoS One* doi: 10.1371/journal.pone.0100042.

D'Angelo, MA, JS Gomez-Cavazos, A Mei, DH Lackner, and MW Hetzer. 2012. "A change in nuclear pore complex composition regulates cell differentiation." *Dev Cell* doi:10.1016/j.devcel.2011.11.021.

Dieppois, G, Iglesias, N, Stutz, F. 2006. "Cotranscriptional recruitment to the mRNA export receptor Mex67p contributes to nuclear pore anchoring of activated genes." *Mol Cell Biol* doi:10.1128/MCB.00870-06.

Dietrich, CR, and GN Newsam. 1997. "Fast and exact simulation of stationary gaussian processes through circulant embedding of the covariance matrix." *SIAM Journal on Scientific Computing* doi:10.1137/S1064827592240555 .

D'Urso, A, Y Takahashi, B Xiong, J Marone, R Coukos, C Randise-Hinchliff, J Wang, A Shilatifard, and JH Brickner. 2016. "Set1/COMPASS and Mediator are repurposed to promote epigenetic transcriptional memory." *eLife* doi:10.7554/eLife.16691.

Egecioglu, DE, A D'Urso, DG Brickner, WH Light, and JH Brickner. 2014. "Approaches to studying subnuclear organization and gene-nuclear pore interactions." *Methods Cell Biol.* doi:10.1016/B978-0-12-417160-2.00021-7.

Falk, M, Y Feodorova, N Naumova, M Imakaev, BR Lajoie, H Leonhardt, B Joffe, et al. 2019. "Heterochromatin drives compartmentalization of inverted and conventional nuclei." *Nature* https://doi.org/10.1038/s41586-019-1275-3.

Femino, AM, FS Fay, K Fogarty, and RH Singer. 1998. "Visualization of single RNA transcripts in situ." *Science* doi:10.1126/science.280.5363.585.

Feng, CM, Y Qiu, EKV Buskirk, EJ Yang, and M Chen. 2014. "Light-regulated gene repositioning in Arabidopsis." *Nat Commun* doi:10.1038/ncomms4027.

Feuerbach, F, Galy, V, Trelles-Sticken, E, Fromont-Racine, M, Jacquier, A, Gilson, E, Olivo-Marin, JC, Scherthan, H, Nehrbass, U. 2002. "Nuclear architecture and spatial positioning help establish transcriptional states of telomeres in yeast." *Nat Cell Biol* doi:10.1038/ ncb756.

Franks, TM, A McCloskey, MN Shokirev, C Benner, A Rathore, and MW Hetzer. 2017. "Nup98 recruits the Wdr82-Set1 A/COMPASS complex to promoters to regulate H3K4 trimethylation in hematopoietic progenitor cells." *Gene Dev* doi:10.1101/gad.306753.117.

Frey, S, and D Gorlich. 2007. "A saturated FG-repeat hydrogel can reproduce the permeability properties of nuclear pore complexes." *Cell* doi:10.1016/j.cell.2007.06.024.

Frey, S, RP Richter, and D Gorlich. 2006. "FG-Rich repeats of nuclear pore proteins form a Three-Dimensional meshwork with Hydrogel-Like properties." *Science* doi:10.1126/science.1132516.

Gall, JG. 1967. "Octagonal nuclear pores." *J Cell Biol* 10.1083/jcb.32.2.391.

Gehlen, LR, G Gruenert, MB Jones, CD Rodley, J Langowski, and JM O'Sullivan. 2012. "Chromosome positioning and the clustering of functionally related loci in yeast is driven by chromosomal interactions." *Nucleus* doi:10.4161/nucl.20971.

Goldberg, MW, Allen, TD. 1992. "High resolution scanning electron microscopy of the nuclear envelope: demonstration of a new, regular, fibrous lattice attached to the baskets of the nucleoplasmic face of the nuclear pores." *J Cell Biol* 10.1083/jcb.119.6.1429.

Gotta, M, Laroche, T, Formenton, A, Maillet, L, Scherthan, H, Gasser, SM. 1996. "The clustering of telomeres and colo- calization with Rap1, Sir3, and Sir4 proteins in wild-type Saccharomyces cerevisiae." *J Cell Biol* doi:10.1083/jcb.134.6.1349.

Gottschling, DE, Aparicio, OM, Billington, BL, Zakian, VA. 1990. "Position effect at S. cerevisiae telomeres: reversible repression of Pol II transcription." *Cell* doi:10.1016/0092-8674(90)90141-Z.

Gough, SM, CI Slape, and PD Aplan. 2011. "NUP98 gene fusions and hematopoietic malignancies: common themes and new biologic insights." *Blood* doi:10 .1182/blood-2011-07-328880.

Gozalo, A, Duke, A, Lan, Y, Pascual-Garcia, P, Talamas, JA, Nguyen, SC, Shah, PP, Jain R, Joyce, EF, Capelson, M. 2020. "Core components of the nuclear pore bind distinct states of chromatin and contribute to Polycomb repression." *Mol Cell* doi:10.1016/j.molcel .2019.10.017.

Green, EM, Y Jiang, R Joyner, and K Weis. 2012. "A negative feedback loop at the nuclear periphery regulates GAL gene expression." *Mol Biol Cell* doi:10 .1091/mbc.e11-06-0547.

Greenberg, ML, P Goldwasser, and SA Henry. 1982. "Characterization of a yeast regulatory mutant constitutive for synthesis of inositol-1-phosphate synthase. Molecular and General Genetics MGG." *Molecular and General Genomics* 186:157–163.

Griffis, ER, Altan, N, Lippincott-Schwartz, J, Powers, MA. 2002. "Nup98 is a mobile nucleoporin with transcription-dependent dynamics." *Mol Biol Cell* doi:10.1091/mbc.01-11-0538.

Guggenberger, T, G Pagnini, T Vojta, and R Metzler. 2019. "Fractional brownian motion in a finite interval: correlations effect depletion or accretion zones of particles near boundaries." *New Journal of Physics* 21:022002.

Guglielmi, V, S Sakuma, and MA D'Angelo. 2020. "Nuclear pore complexes in development and tissue homeostasis." *Development* doi:10.1242/dev.183442.

Haeusler, RA, M Pratt-Hyatt, PD Good, TA Gipson, and DR Engelke. 2008. "Clustering of yeast tRNA genes is mediated by specific association of condensin with tRNA gene transcription complexes." *Genes & Development* doi:10.1101/gad.1675908.

Hajjoul, H, J Mathon, H Ranchon, I Goiffon, J Mozziconacci, B Albert, P Carrivain, et al. 2013. "High-throughput chromatin motion tracking in living yeast reveals the flexibility of the fiber throughout the genome." *Genome Research* doi:10.1101/gr.157008.113.

Hansen, AS, N Hao, and EK O'Shea. 2018. "High-throughput microfluidics to control and measure signaling dynamics in single yeast cells." *Nature Protocol* doi: 10.1038/nprot.2015.079.

Hediger, F, AS Berthiau, G van Houwe, E Gilson, and SM Gasser. 2006. "Subtelomeric factors antagonize telomere anchoring and Tel1-independent telomere length regulation." *The EMBO Journal* doi:10.1038/sj.emboj.7600976 .

Hediger, F, FR Neumann, G Van Houwe, K Dubrana, and SM Gasser . 2002. "Live imaging of telomeres: yku and sir proteins define redundant telomere-anchoring pathways in yeast." *Current Biology* 12:2076–2089.

Heyken, WT, A Repenning, J Kumme, and HJ Schuller. 2005. "Constitutive expression of yeast phospholipid biosynthetic genes by variants of Ino2 activator defective for interaction with Opi1 repressor." *Molecular Microbiology* doi:10.1111/j.1365-2958.2004.04499.

Hnisz, D, K Shrinivas, RA Young, AK Chakraborty, and PA Sharp. 2017. "A phase separation model for transcriptional control." *Cell* doi:10.1016/j.cell.2017.02.007.

Hope, IA, and K Struhl. 1985. "GCN4 protein, synthesized in vitro, binds HIS3 regulatory sequences: implications for general control of amino acid biosynthetic genes in yeast." *Cell* doi:10.1016/0092-8674(85) 90022-4.

Hou, S, J Exell, and K Welsher. 2020. "Real-time 3D single molecule tracking." *Nat Commun* doi: 10.1038/s41467-020-17444-6.

Hult, C, D Adalsteinsson, PA Vasquez, J Lawrimore, M Bennett, A York, D Cook, E Yeh, MG Forest, and K Bloom. 2017. "Enrichment of dynamic chromosomal crosslinks drive phase separation of the nucleolus." *Nucleic Acids Research* doi:10.1093/nar/gkx741.

Ibarra, A, C Benner, S Tyagi, J Cool, and MW Hetzer. 2016. "Nucleoporin-mediated regulation of cell identity genes." *Genes Dev* doi:10.1101/gad.287417.116.

Jacinto, FV, Benner, C, Hetzer, MW. 2015. "The nucleoporin Nup153 regulates embryonic stem cell pluripotency through gene silencing." *Gene Dev* doi:10.1101/gad.260919.115.

Jani, D, Valkov E, Stewart, M. 2014. "Structural basis for binding the TREX2 complex to nuclear pores, GAL1 localisation and mRNA export." *Nucleic Acids Res* doi:10.1093/nar/gku252.

Jost, KL, B Bertulat, and MC Cardoso. 2012. "Heterochromatin and gene positioning: inside, outside, any side?" *Chromosoma.*

Kadota, S, J Ou, Y Shi, JT Lee, J Sun, and E Yildirim. 2020. "Nucleoporin 153 links nuclear pore complex to chromatin architecture by mediating CTCF and cohesin binding." *Nat Commun* doi:10.1038/s41467- 020-16394-3.

Kaltenbach, S, G Soler, C Barin, C Gervais, OA Bernard, V Penard-Lacronique, and SP Romana. 2010. "NUP98- MLL fusion in human acute myeloblastic leukemia." *Blood* doi:10.1182/blood-2010-04- 277806.

Kalverda, B, Pickersgill, H, Shloma, VV, Fornerod, M. 2010. "Nucleoporins directly stimulate expression of developmental and cell-cycle genes inside the nucleoplasm ." *Cell* doi:10.1016/j.cell.2010.01.011.

Kapoor, P, M Chen, DD Winkler, K Luger, and X Shen. 2013. "Evidence for monomeric actin function in INO80 chromatin remodeling." *Nature Structural & Molecular Biology* doi:10.1038/nsmb.2529.

Kashkanova, AD, AB Shkarin, RG Mahmoodabadi, M Blessing, Y Tuna, A Gemeinhardt, and V Sandoghdar. 2021. "Precision single-particle localization using radial variance transform." *Opt. Express* doi: 10.1364/OE.420670.

Khanna, N, Y Zhang, JS Lucas, OK Dudko, and C Murre. 2019. "Chromosome dynamics near the sol-gel phase transition dictate the timing of remote genomic interactions." *Nat Comm* doi: 10.1038/s41467-019-10628-9.

Kim, S, I Liachko, DG Brickner, K Cook, WS Noble, JH Brickner, J Shendure, and MJ Dunham. 2017. "The dynamic three-dimensional organization of the diploid yeast genome." *eLife* doi:10.7554/ eLife.23623.

Kim, S, MJ Dunham, and J Shendure. 2019. "A combination of transcription factors mediates inducible interchromosomal contacts." *eLife* doi:10.7554/eLife.42499.

Kuhn, TM, P Pascual-Garcia, A Gozalo, SC Little, and M Capelson. 2019. "Chromatin targeting of nuclear pore proteins induces chromatin decondensation." *J Cell Biol* doi:10.1083/jcb.201807139.

Lapetina, DL, Ptak, C, Roesner, UK, Wozniak, RW. 2017. "Yeast silencing factor Sir4 and a subset of nucleoporins form a complex distinct from nuclear pore complexes." *J Cell biol* doi:10.1083/jcb.201609049.

Larsson, AJM, P Johnsson, M Hagemann-Jensen, L Hartmanis, OR Faridani, B Reinius, A Segerstolpe, CM Rivera, B Ren, and R Sandberg. 2019. "Genomic encoding of transcriptional burst kinetics." *Nature* doi:10.1038/ s41586-018-0836-1.

Liang, Y, TM Franks, MC Marchetto, FH Gage, and MW Hetzer. 2013. "Dynamic association of NUP98 with the human genome." *PLoS Genet* doi:10.1371/journal.pgen.1003308.

Light, WH, DG Brickner, VR Brand, and JH Brickner. 2010. "Interaction of a DNA zip code with the nuclear pore complex promotes H2A.Z incorporation and INO1 transcriptional memory." *Mol Cell* doi:10.1016/j.molcel.2010.09.007.

Light, WH, J Freaney, V Sood, A Thompson, A D'Urso, CM Horvath, and JH Brickner. 2013. "A conserved role for human Nup98 in altering chromatin structure and pro- moting epigenetic transcriptional memory." *Plos Biol* doi:10.1371/journal.pbio.1001524.

Lin, D. H., Hoelz, A. 2019. "The Structure of the Nuclear Pore Complex (An Update)." *Annual review of biochemistry* doi:10.1146/annurev-biochem-062917-011901.

Lucas, JS, Y Zhang, OK Dudko, and C Murre. 2014. "3d trajectories adopted by coding and regulatory DNA elements: first-passage times for genomic interactions." *Cell* doi:10.1016/j.cell.2014.05.036.

Luthra, R, SC Kerr, MT Harreman, LH Apponi, MB Fasken, S Ramineni, S Chaurasia, SR Valentini, and AH Corbett. 2007. "Actively transcribed GAL genes can be physically linked to the nuclear pore by the SAGA chromatin modifying complex." *J Biol Chem* doi:10.1074/jbc.M608741200.

Mandelbrot, BB, and JW Van Ness. 1968. "Fractional brownian motions, fractional noises and applications." *SIAM* doi:10.1137/1010093.

Marshall, WF, A Straight, JF Marko, J Swedlow, A Dernburg, A Belmont, AW Murray, DA Agard, and JW Sedat. 1997. "Interphase chromosomes undergo constrained diffusional motion in living cells." *Curr Biol* doi:10.1016/S0960-9822(06)00412-X.

Meyer, Y, F Sellan, and MS Taqqu. 1999. "Wavelets, generalized white noise and fractional integration: the synthesis of fractional brownian motion." *The Journal of Fourier Analysis and Applications* doi:10.1007/BF01261639 .

Michmerhuizen, NL, JM Klco, and CG Mullighan. 2020. "Mechanistic insights and potential therapeutic approaches for NUP98-rearranged hematologic malignancies." *Blood* doi:10.1182/blood.2020007093.

Mine-Hattab, J, and R Rothstein. 2013. "DNA in motion during double-strand break repair." *Trends in Cell Biology* doi:10.1016/j.tcb.2013.05.006.

Misteli, T. 2020. "The Self-Organizing Genome: Principles of Genome Architecture and Function." *Cell* doi:10.1016/j.cell.2020.09.014.

Mueller, PP, and AG Hinnebusch. 1986. "Multiple upstream AUG codons mediate translational control of GCN4." *Cell* doi:10.1016/0092-8674(86)90384-3.

Mueller, PP, S Harashima, and AG Hinnebusch. 1987. "A segment of GCN4 mRNA containing the upstream AUG codons confers translational control upon a heterologous yeast transcript." *PNAS* doi:10.1073/pnas.84.9.2863 .

Noma, K, HP Cam, RJ Maraia, and SI Grewal. 2006. "A role for TFIIIC transcription factor complex in genome organization." *Cell* doi:10.1016/j.cell.2006.04.028.

Pascual-Garcia, P, B Debo, JR Aleman, JA Talamas, Y Lan, NH Nguyen, KJ Won, and M Capelson. 2017. "Metazoan nuclear pores provide a scaffold for poised genes and mediate induced enhancer–promoter contacts." *Mol Cell* doi:10.1016/j.molcel.2017.02.020.

Pascual-Garcia, P, J Jeong, and M Capelson. 2014. "Nucleoporin Nup98 associates with Trx/MLL and NSL histone-modifying complexes and regulates Hox gene expression." *Cell Rep* doi:10.1016/j.celrep.2014.09.002.

Ptak, C, JD Aitchison, and RW Wozniak. 2014. "The multifunctional nuclear pore complex: a platform for controlling gene expression." *Current opinion in cell biology* doi:10.1016/j.ceb.2014.02.001.

Quinodoz, SA, N Ollikainen, B Tabak, A Palla, JM Schmidt, E Detmar, MM Lai, et al. 2018. " Higher-Order Inter-chromosomal Hubs Shape 3D Genome Organization in the Nucleus." *Cell* doi: 10.1016/j.cell.2018.05.024.

Raices, M, L Bukata, S Sakuma, J Borlido, LS Hernandez, DO Hart, and MA D'Angelo. 2017. "Nuclear pores regulate muscle development and maintenance by assembling a localized Mef2C complex." *Dev Cell* doi:10.1016/j.devcel.2017.05.007.

Ramos, E, D Ghosh, E Baxter, and VG Corces. 2006. "Genomic organization of gypsy chromatin insulators in Drosophila melanogaster." *Genetics* doi:10.1534/genetics.105.054742.

Randise-Hinchliff, C, R Coukos, V Sood, MC Sumner, S Zdraljevic, L Meldi-Sholl, DG Brickner, S Ahmed, L Watchmaker, and JH Brickner. 2016. "Strategies to regulate transcription factor–mediated gene positioning and interchromosomal clustering at the nuclear periphery." *Journal of Cell Biology* doi:10.1083/jcb.201508068.

Rawal, Y, RV Chereji, V Valabhoju, H Qiu, J Ocampo, DJ Clark, and AG Hinnebusch. 2018. "Gcn4 binding in coding regions can activate internal and canonical 50 promoters in yeast." *Mol Cell* doi:10.1016/j.molcel.2018.03.007.

Roberts, SM, and F Winston. 1997. "Essential functional interactions of SAGA, a Saccharomyces cerevisiae complex of Spt, Ada, and Gcn5 proteins, with the Snf/Swi and Srb/mediator complexes." *Genetics* 147:451–465.

Rodriguez, J, and DR Larson. 2020. "Transcription in living cells: molecular mechanisms of bursting." *Annual Review of Biochemistry* doi:10.1146/annurev-biochem-011520-105250.

Rodríguez-Navarro, S, T Fischer, MJ Luo, O Antúnez, S Brettschneider, J Lechner, JE Pérez-Ortín, R Reed, and E Hurt. 2004. "Sus1, a functional component of the SAGA histone acetylase complex and the nuclear pore-associated mRNA export machinery." *Cell* doi:10.1016/S0092-8674(03)01025-0.

Sabari, BR, A Dall'Agnese, A Boija, IA Klein, EL Coffey, K Shrinivas, BJ Abraham, et al. 2018. "Coactivator condensation at super-enhancers links phase separation and gene control." *Science* doi:10.1126/science.aar3958.

Salem, A, and M Alnegga. 2020. "Fractional Langevin equations with multi-point and non-local integral boundary conditions." *Cogent Mathematics & Statistics* doi: 10.1080/25742558.2020.1758361 .

Smith, S, C Galinha, S Desset, F Tolmie, D Evans, C Tatout, and K Graumann. 2015. "Marker gene tethering by nucleoporins affects gene expression in plants." *Nucleus* doi:10.1080/19491034.2015.1126028.

Sood, V, I Cajigas, A D'Urso, WH Light, and JH Brickner. 2017. "Epigenetic transcriptional memory of GAL genes depends on growth in glucose and the Tup1 transcription factor in Saccharomyces cerevisiae." *Genetics* doi:10.1534/genetics.117.20163.

Strambio-De-Castillia, C, M Niepel, and MP Rout. 2010. "The nuclear pore complex: bridging nuclear transport and gene regulation." *Nat. Rev. Mol. Cell Biol.* doi:10.1038/nrm2928.

Taddei, A, G Van Houwe, S Nagai, I Erb, E van Nimwegen, and SM Gasser. 2009. "The functional importance of telomere clustering: global changes in gene expression result from SIR factor dispersion." *Genome Research* doi:10.1101/gr.083881.108.

Texari, L, G Dieppois, P Vinciguerra, MP Contreras, A Groner, A Letourneau, and F Stutz. 2013. "The nuclear pore regulates GAL1 gene transcription by controlling the localization of the SUMO protease Ulp1." *Mol Cell* doi:10.1016/j.molcel.2013.08.047.

Thompson, M, RA Haeusler, PD Good, and DR Engelke. 2003. "Nucleolar clustering of dispersed tRNA genes." *Science* doi:10.1126/science.1089814.

Tunnacliffe, E, AM Corrigan, and JR Chubb. 2018. "Promoter-mediated diversification of transcriptional bursting dynamics following gene duplication." *Proc National Acad Sci* doi:10.1073/pnas.1800943115.

Tutucci, E., Vera, M., Biswas, J., Garcia, J., Parker, R., Singer, R. H. 2018. "An improved MS2 system for accurate reporting of the mRNA life cycle." *Nature methods* doi: 10.1038/nmeth.4502.

Vallotton, P, S Rajoo, M Wojtynek, E Onischenko, A Kralt, CP Derrer, and K Weis. 2019. "Mapping the native organization of the yeast nuclear pore complex using nuclear radial intensity measurements." *PNAS* 116:14606–14613.

Van de Vosse, DW, Wan ,Y, Lapetina, DL, Chen, WM, Chiang, JH, Aitchison, JD, Wozniak, RW. 2013. "A role for the nucleoporin Nup170p in chromatin structure and gene silencing." *Cell* doi:10.1016/j.cell.2013.01.049.

Verdaasdonk, JS, PA Vasquez, RM Barry, T Barry, S Goodwin, MG Forest, and K Bloom. 2013. "Centromere tethering confines chromosome domains." *Mol Cell* doi:10.1016/j.molcel.2013.10.021.

Vojta, T, and A Warhover. 2021. "Probability density of fractional Brownian motion and the fractional Langevin equation with absorbing walls." *Journal of Statistical Mechanics: Theory and Experiment* doi: 10.1088/1742-5468.

Vojta, T, S Halladay, S Skinner, S Januaonis, T Guggenberger, and R Metzler. 2020. "Reflected fractional Brownian motion in one and higher dimensions." *Physical Review E* doi:10.1103/PhysRevE.

Vojta, T, S Skinner, and R Metzler. 2019. "Probability density of the fractional Langevin equation with reflecting walls." *Phy Rev E* doi:0.1103/PhysRevE.100.042142.

von Appen, A, Beck, M. 2016. ". Structure determination of the nuclear pore complex with three-dimensional cryo electron microscopy." *J Mol Biol* 10.1016/ j.jmb.2016.01.004.

Wang, A, JA Kolhe, N Gioacchini, I Baade, WM Brieher, CL Peterson, and BC Freeman. 2020. "Mechanism of Long Range Chromosome Motion Triggered by Gene Activation." *Developmental Cell* doi:10.1016/j.devcel.2019.12.007 .

Watson, ML. 1955. "The nuclear envelope its structure and relation to cytoplasmic membranes." *J Biophys Biochem Cytol* 10.1083/jcb.1.3.257 .

Weiler, KS, Wakimoto, BT. 1995. "Heterochromatin and gene expression in Drosophila." *Annu Rev Genet* doi:10.1146/annurev.ge.29.120195.003045.

Wood, EJ, T Maniatis, EF Fritsch, and J Sambrook. 1983. "Molecular Cloning: A Laboratory Manual." *Cold Spring Harbor Laboratory.*

Xu, M, and PR Cook. 2008. "Similar active genes cluster in specialized transcription factories." *Journal of Cell Biology* doi:10.1083/jcb.200710053.

Yang, Q, MP Rout, and CW Akey. 1998. "Three-Dimensional architecture of the isolated yeast nuclear pore complex: functional and evolutionary implications." *Molecular Cell* doi:10.1016/s1097-2765.

Zykova, TY, VG Levitsky, ES Belyaeva, and IF Zhimulev. 2018. "Polytene chromosomes—a portrait of functional organi- zation of the Drosophila genome." *Current Genomics* doi:10.2174/1389202918666171016123830.

VITA

Michael Chas Sumner was born in Boca Raton, Florida, USA, on September 29th, 1992, to Bette Jane Sumner and Charles Sumner. Being raised within proximity to the Everglades and the Atlantic Ocean afforded Chas the opportunity to learn about the unique ecology that surrounded him, leading to a job at the Gumbo Limbo Nature Center during high school. This interest expanded to a fascination with the biological research being conducted at Gumbo Limbo. In 2011, Chas enrolled at the University of Rochester as a Biochemistry major. He would go on to change his major multiple times before declaring a Cell and Developmental Biology major with a Chemistry minor at the end of his second year. That summer, Chas began working in a few labs before joining the Cohen Lab at the University of Rochester Medical Center. His projects involved biochemical assays, fluorescent microscopy, and mouse dissections. This led Chas to his love of fluorescence imaging and a strong desire to work with microbes as a model organism. In 2015, Chas enrolled in Northwestern University's Interdisciplinary Biological Sciences Ph.D. program. Chas has accepted a job offer with Illumina as a Scientist 1 in Assay Development, and will move to San Diego shortly after receiving his Ph.D.